1995ApJ...445..108T

THE ASTROPHYSICAL JOURNAL, 445:108–123, 1995 May 20
© 1995. The American Astronomical Society. All rights reserved. Printed in U.S.A.

HEAVY ELEMENT ABUNDANCES IN A NEW SAMPLE OF LOW-METALLICITY BLUE COMPACT GALAXIES

TRINH X. THUAN[1]
Astronomy Department, University of Virginia, Charlottesville, VA 22903; DAEC, Observatoire de Paris-Meudon, Meudon; and Service d'Astrophysique, Centre d'Études de Saclay

YURI I. IZOTOV
Main Astronomical Observatory, Ukrainian Academy of Sciences, Goloseevo, Kiev 252127, Ukraine

AND

VALENTIN A. LIPOVETSKY[1]
Special Astrophysical Observatory, Russian Academy of Sciences, Nizhny Arkhyz, Karachai-Circessia 357147, Russia
Received 1994 April 14; accepted 1994 December 1

ABSTRACT

We present high-quality spectrophotometric observations of 15 supergiant H II regions in 14 new low-metallicity blue compact galaxies (BCGs) selected mainly from the First and Second Byurakan Surveys and with oxygen abundance 12 + log O/H between 7.37 and 8.04 ($Z_\odot/35 \leq Z \leq Z_\odot/7$). We use the data to determine abundances for the elements N, O, Ne, S, Ar, and, for the first time in BCGs, Fe; discuss their origin; and constrain current nucleosynthesis stellar models.

The main result of the present study is that *none* of the heavy element–to–oxygen abundance ratios studied here (N/O, Ne/O, S/O, Ar/O, Fe/O) depend on oxygen abundance. We conclude that all these heavy elements have a primary origin and are produced by the same massive ($M \geq 10\ M_\odot$) stars. The dispersion of the N/O ratio is found to be remarkably small, being only ± 0.08 in the log. This can only be understood if primary N is produced in massive stars, *not* in intermediate-mass ($4\ M_\odot \leq M \leq 9\ M_\odot$) stars as commonly thought. BCGs show the same O/Fe overabundance with respect to the Sun ($\sim$0.34 in the log) as galactic halo stars, suggesting the same chemical enrichment history, and supporting the scenario of an early enrichment of the galactic halo by massive Population III stars.

We have compared the observed heavy element abundance ratios with theoretical yields from current massive star nucleosynthesis models from Weaver & Woosley (1993). The small dispersion in the heavy element abundance ratios suggests that there is *not* a large IMF variation between BCGs with different metallicities.

Subject headings: galaxies: abundances — galaxies: compact — H II regions — nuclear reactions, nucleosynthesis, abundances

1. INTRODUCTION

The study of the relative variations of one chemical element relative to another is crucial for our understanding of the chemical evolution of galaxies and for constraining models of stellar nucleosynthesis and the shape of the stellar initial mass function (IMF). Blue compact galaxies (BCGs) are ideal objects in which to carry out such a study. They are undergoing intense bursts of star formation which give birth to a large number (10^3–10^4) of massive stars in a compact region, which ionize the interstellar medium, producing high-excitation supergiant H II regions, and enrich it with heavy elements (see Thuan 1991 for a review). The optical spectra of these H II regions show strong narrow emission lines superposed on a stellar continuum which is rising toward the blue, allowing abundance determination of such heavy elements as nitrogen, oxygen, neon, sulfur, argon or, as done for the first time in this paper for BCGs, iron. Moreover, BCGs have a high neutral hydrogen content (Thuan & Martin 1981) and are metal deficient with respect to the solar neighborhood ($Z_\odot/50 \leq Z \leq Z_\odot/3$) suggesting that they are relatively young from the point of view of chemical evolution (Thuan 1991). Thus they are excellent laboratories for studying nucleosynthesis processes in a metal-deficient environment, in conditions similar to those prevailing at the time of galaxy formation.

It is now well established theoretically that the oxygen seen in H II regions is a primary element produced by massive stars with $M \geq 10\ M_\odot$ (Burbidge et al. 1957; Cameron 1957; Arnett 1978; Maeder 1992; Weaver & Woosley 1993). These predictions have been confirmed by many studies of abundances in stars (Conti et al. 1967; Clegg, Lambert, & Tomkin 1981; Wheeler, Sneden, & Truran 1989). As for the other α-process elements seen in the spectra of H II regions, such as neon, argon, and sulfur, they are generally thought to be also primary. The neon-to-oxygen abundance ratio is known not to be dependent on oxygen abundance (Vigroux, Stasinska, & Comte 1987), implying that both elements are made by the same massive stars. As for sulfur, Garnett (1989) also found a constant S/O ratio, independent of O/H, in his study of H II regions in dwarf irregulars and BCGs. This is at variance with the results of Shaver et al. (1983), Evans (1986), and Vilchez et al. (1988) who found in their studies of H II regions in nearby spiral galaxies radial gradients in the S/O ratio, in the sense of a larger S/O ratio in H II regions with lower O/H. Garnett (1989) has argued that these gradients are not real but are caused by the use of incorrect ionization correction factors

[1] Visiting Astronomer, Kitt Peak National Optical Observatories, operated by the Association of Universities for Research in Astronomy, Inc., under contract with the National Science Foundation.

© American Astronomical Society • Provided by the NASA Astrophysics Data System

1995ApJ...445..108T

(ICFs). These ICFs are difficult to determine because of their complex dependence on the adopted stellar atmosphere models for massive stars. Argon is also thought to be a primary element. The Ar/O ratio is also observed to be independent of O/H in the cool low-excitation H II regions in nearby spiral galaxies (Stevenson, McCall, & Welch 1993 and references therein), although argon abundances are not very well determined because of the uncertainties in the ICFs and the weakness of the Ar III and Ar IV lines.

The situation for nitrogen is more complex. Spectral observations of H II regions in spiral galaxies with high metallicities ($Z \sim Z_{\odot}$) show that the N/O ratio increases with O/H (Pagel & Edmunds 1981; Serrano & Peimbert 1983; Torres-Peimbert, Peimbert, & Fierro 1989; Vila-Costas & Edmunds 1993). This implies that a large part of the nitrogen in these high-metallicity spiral galaxies is produced as a secondary element in the CNO cycle, i.e., its synthesis is controlled by carbon seed atoms already present in the main-sequence or red giant star (which can be of any mass). However, in low-metallicity ($Z_{\odot}/50 \leq Z \leq Z_{\odot}/3$) environments such as in irregular and blue compact galaxies, the N/O ratio is found to be constant and independent of O/H (Lequeux et al. 1979; French 1980; Kinman & Davidson 1981; Kunth & Sargent 1983; Campbell, Terlevich, & Melnick 1981). This implies that nitrogen is mainly a primary element when O/H is small. Conventional stellar nucleosynthesis models predict that primary nitrogen is produced mainly in intermediate-mass ($3\ M_{\odot} \leq M \leq 9\ M_{\odot}$) stars by hot-bottom carbon burning undergoing a third dredge-up episode which brings carbon-rich material from the core into the hydrogen-burning shell (Renzini & Voli 1981). The spread of the N/O ratio at a fixed O/H is seen to be large and has been attributed to observational uncertainties and/or to the time delays ($\tau \leq 5 \times 10^8$ yr) between the production of oxygen by short-lived massive stars and that of nitrogen by longer lived intermediate-mass stars (Matteucci & Tosi 1985; Garnett 1990; Pilyugin 1992, 1993; Vila-Costas & Edmunds 1993; Marconi, Matteucci, & Tosi 1994).

The optical spectra of BCGs also contain iron lines, allowing us to derive abundances of that element. Iron is a primary element produced during explosive nucleosynthesis either in Type I supernovae (SN I's) with low-mass progenitors or in Type II supernovae (SN II's) with more massive progenitors (Weaver & Woosley 1993). Due to the difference in evolution timescales of Type I and Type II supernova progenitors, SN I's begin to contribute only when the age of system is $\geq 10^9$ yr. During the collapse of the Galaxy, while O and other α-elements are mainly produced in massive stars and restored to the interstellar medium (ISM) through SN II's, iron is thought to come mainly from SN I's at later stages of the Galaxy's evolution. Therefore, oxygen is injected sooner than iron into the ISM, resulting in an oxygen overabundance relative to iron in the halo population. It is well established that halo Population II stars with [Fe/H] < -1 (where [X] $\equiv \log X - \log X_{\odot}$) have a constant overabundance [O/Fe] $\sim$ 0.3–0.5. As for disk stars with higher metallicities ([Fe/H] ≥ -1), they show a progressive drop of O/Fe toward the solar ratio ([O/Fe] ~ 0) (Lambert, Sneden, & Ries 1974; Gratton & Ortolani 1986; Barbuy 1988; Barbuy & Erdelyi-Mendes 1989; Spite & Spite 1991; Bessel, Sutherland, & Ruan 1991; Edvardsson et al. 1993).

On the theoretical front, there remain uncertainties concerning models of explosive nucleosynthesis (Woosley & Weaver 1986; Mayle & Wilson 1988; Shigeyama, Nomoto, & Hashimoto 1988; Woosley 1988; Bruenn 1989; Thielemann, Hashimoto, & Nomoto 1990; Weaver & Woosley 1993; Woosley, Langer, & Weaver 1993). The central collapsing core parameters and initial conditions for the shock wave are still being debated, casting uncertainty on the iron yield which depends sensitively on these parameters.

In order to constrain models of stellar nucleosynthesis and chemical evolution of the heavy elements discussed above in a metal-deficient environment, we present in this paper high signal-to-noise ratio spectrophotometric observations of 15 H II regions in 14 low-metallicity ($Z_{\odot}/35 \leq Z \leq Z_{\odot}/7$) BCGs. In § 2, we describe the observations and data reduction. In § 3, we determine the physical conditions, the heavy element abundances, and yields in the BCG star-forming regions. In § 4, we compare our observational results with models of stellar nucleosynthesis to constrain their parameters. We summarize our conclusions in § 5. Preliminary results of this work have been reported by Thuan et al. (1994).

2. OBSERVATIONS AND DATA REDUCTION

High signal-to-noise ratio spectrophotometric observations (S/N $\sim$ 20–50 in the continuum at 5000 Å) of 15 H II regions in 14 BCGs were obtained with the Kitt Peak 4 m Mayall telescope on the nights of 1993 March 23–24. Twelve BCGs were selected from a complete sample of $\sim$450 BCGs (Izotov et al. 1992b) discovered in the First and the Second Byurakan objective prism surveys (Markarian 1967; Markarian, Lipovetsky, & Stepanian 1983; Markarian et al. 1989). They were chosen to have metallicity lower than $\sim Z_{\odot}/10$, as estimated from low signal-to-noise ratio Russian 6 m telescope spectra. Two additional galaxies, UGC 4483 $\equiv$ 0832+699 (Izotov et al. 1992a) and CG 389 $\equiv$ 1415+437, were also included because of the low metal content ($Z \leq Z_{\odot}/20$) of their brightest H II regions. The general properties of the observed galaxies are given in Table 1. One galaxy, 1331+493, has two H II regions, which we designate by 1331+493 and 1331+493S.

All observations were made with the Ritchey-Chrétien RC2 spectrograph used in conjunction with the T2KB 2048 × 2048 CCD detector. We use a 2″ × 300″ slit with the KPC-10A grating (316 lines mm^{-1}) in first order, with a GG 385 order separation filter. This filter cuts off all second-order contamination for wavelengths blueward of 7200 Å which is the wavelength region of interest here. The above instrumental set-up gave a spatial scale along the slit of 0″.69 pixel^{-1}, a scale perpendicular to the slit of 3.7 Å pixel^{-1}, a spectral range of 3500–7500 Å, and a spectral resolution of $\sim$7 Å. These parameters permitted us to cover simultaneously the blue and red spectral range with all the lines of interest in a single exposure and with enough spectral resolution to separate important emission lines as Hγ λ4340 and [O III] λ4363, and Hα λ6563 and [N II] λ6584. The seeing was typically 1″.5–2″. Both nights were transparent, so that absolute spectrophotometry was possible. Total exposure times varied between 30 and 60 minutes. They were broken up into two or three subexposures to allow for cosmic-ray removal. All objects were observed at airmasses less than 1.3, so that no corrections were made for atmospheric dispersion. Three Kitt Peak IRS spectrophotometric standard stars were observed each night for flux calibration. Spectra of He–Ne–Ar comparison arcs were obtained before and after each observation to calibrate the wavelength scale. A summary of the observations is given in Table 2.

The details of the data reduction are given in Paper I (Izotov, Thuan, & Lipovetsky 1994), where the results of the

© American Astronomical Society • Provided by the NASA Astrophysics Data System

1995ApJ...445..108T

TABLE 1

GENERAL PARAMETERS OF GALAXIES

Name	Coordinates (1950.0) α	δ	m_{pg}	Angular diameter[a]	z	M^{b}_{pg}	Other names[c]	Ref.[d]
0832+699	$08^h32^m00.0^s$	+69°54′00″	14.9	10[e]	0.0009	−12.9	UGC 4483	1
0940+544N	09 40 50.4	+54 25 28	17.3	4	0.0055	−14.7		2
0946+558	09 46 03.1	+55 48 46	15.8	13×17	0.0053	−15.8	Mrk 22	2,3
0948+532	09 48 16.7	+53 13 00	18.0	6	0.0463	−18.5		2
1135+581	11 35 51.3	+58 09 24	15.5	13	0.0034	−15.2	Mrk 1450	2,4
1152+579	11 52 52.1	+57 56 26	16.5	7	0.0172	−17.7	Mrk 193	5
1159+545	11 59 29.0	+54 32 33	18.0	5	0.0119	−15.5		2
1211+540	12 11 33.9	+54 01 58	17.8	8	0.0031	−12.9		2
1249+493	12 49 35.8	+49 19 45	17.5	6	0.0245	−17.6		2
1331+493	13 31 20.4	+49 21 35	15.0	24×18	0.0020	−15.2		2
1331+493S	13 31 20.4	+49 21 35	15.0	24×18	0.0020	−15.2		1,2
1415+437	14 15 03.4	+43 43 42	16.0	25×10	0.0016	−14.0	CG 389	6
1420+544	14 20 59.1	+54 27 42	18.5	6	0.0206	−16.6	SBS, CG 413	2
1437+370	14 37 03.0	+37 01 07	17.0	10	0.0014	−12.9	Mrk 475	7
1533+469	15 33 23.9	+46 58 46	16.5	15×10	0.0189	−17.9		2

[a] In arcseconds.

[b] All objects are assumed to be at their redshift distances with $H_0 = 75$ km s^{-1} Mpc^{-1}.

[c] Blank entries are SBS objects.

[d] REFERENCES.—(1) Izotov et al. 1992a; (2) Izotov et al. 1991, 1992b; (3) Markarian 1967; (4) Markarian, Lipovetsky, & Stepanian 1981; (5) Markarian 1969; (6) Sanduleak & Pesch (1987); (7) Markarian & Lipovetsky 1972.

[e] Diameter of the brightest H II region.

abundance determinations of 10 out of the 15 H II regions in the present sample have been discussed in connection with the primordial helium abundance problem. Briefly, we extracted one-dimensional spectra, using the IRAF and MIDAS software packages, by summing 5 pixel rows along the slit, corresponding to an angular size 3″.5, about the size of the brightest part of the H II regions in our BCG sample. The resulting spectra are shown in Figure 1. We have given here only the spectra of the five H II regions not yet shown in Figures 1 and 2 of Paper I. We refer the reader to the latter paper for the spectra of the remaining H II regions.

As a whole, the H II regions in our BCG sample show high-excitation spectra: 13 have a Hβ equivalent width greater than 100 Å. The spectra of 1331+493S and 1533+469 show more modest excitation, their hydrogen emission lines being on top of strong stellar absorption features characteristic of the late stages of a starburst. We note that, as 0940+544N, 1135+581, and 1152+579 whose spectra were shown in Paper I, 1415+437 and 1420+544 also exhibit a low-intensity (~2% of peak intensity) broad emission component (the full width at zero intensity is ~2000–4000 km s^{-1}) at the base of the Hα line. In 1420+544, the broad component shows a red asymmetry which can be also seen at the base of the Hβ λ4861 and [O III] λ5007 lines. We interpret these low-intensity broad components as due to fast gas motions energized by supernova explosions. The presence of broad components is not necessarily connected with that of Wolf-Rayet features, so they are probably not directly related to stellar winds. A preliminary discussion of the low-intensity broad component phenomenon in BCGs is given in Thuan et al. (1994).

TABLE 2

JOURNAL OF OBSERVATIONS

Galaxy	Date	No. of exp.	Total exp. (min)	Airmass
0832+699	March 23,1993	3	30	1.33
0940+544N	March 24	3	60	1.14
0946+558	March 23	2	30	1.22
0948+532	March 24	1	15	1.08
1135+581	March 24	3	30	1.15
1152+579	March 24	3	45	1.11
1159+545	March 24	3	60	1.11
1211+540	March 23	3	60	1.11
1249+493	March 23	3	55	1.12
1331+493	March 23	3	45	1.18
1331+493S	March 23	3	45	1.18
1415+437	March 24	3	45	1.02
1420+544	March 24	3	55	1.10
1437+370	March 24	2	35	1.08
1533+469	March 23	1	15	1.05

The observed line intensities $F(\lambda)$ normalized to $F(\mathrm{H}\beta)$ for the five H II regions shown in Figure 1 are given in Table 3. Again, the results for the remaining 10 H II regions can be found in Paper I. The line intensities were corrected for both reddening and underlying stellar absorption derived simultaneously by an interactive procedure as described in Paper I. The corrected line intensities $I(\lambda)/I(\mathrm{H}\beta)$, extinction coefficients $C(\mathrm{H}\beta)$, and equivalent widths EW(abs) of the hydrogen absorption stellar lines are also given in Table 3, along with the uncorrected Hβ flux and Hβ equivalent width. In general, $C(\mathrm{H}\beta)$ and EW(abs) are small for the galaxies under study. Our procedure for correcting for absorption works well in most cases, the intensities of the corrected hydrogen lines being in good agreement with the theoretical values (Brocklehurst 1971; Aller 1984). The three exceptions are 0940+544N, 1159+545, and 1331+493S. The first two galaxies have too large a Hγ line intensity and too small a Hα line intensity (Paper I), while the hydrogen line intensities in 1331+493S are uncertain due to strong underlying absorption and the difficulty of defining the continuum.

3. PHYSICAL CONDITIONS AND HEAVY ELEMENT ABUNDANCES AND YIELDS

3.1. *Electron Temperatures and Ionization Correction Factors*

To determine element abundances, we adopt a two-zone photoionized H II region model: a high-ionization zone with temperature T_e(O III), where O III, Ne III, and Ar IV lines orig-

© American Astronomical Society • Provided by the NASA Astrophysics Data System

1995ApJ...445..108T

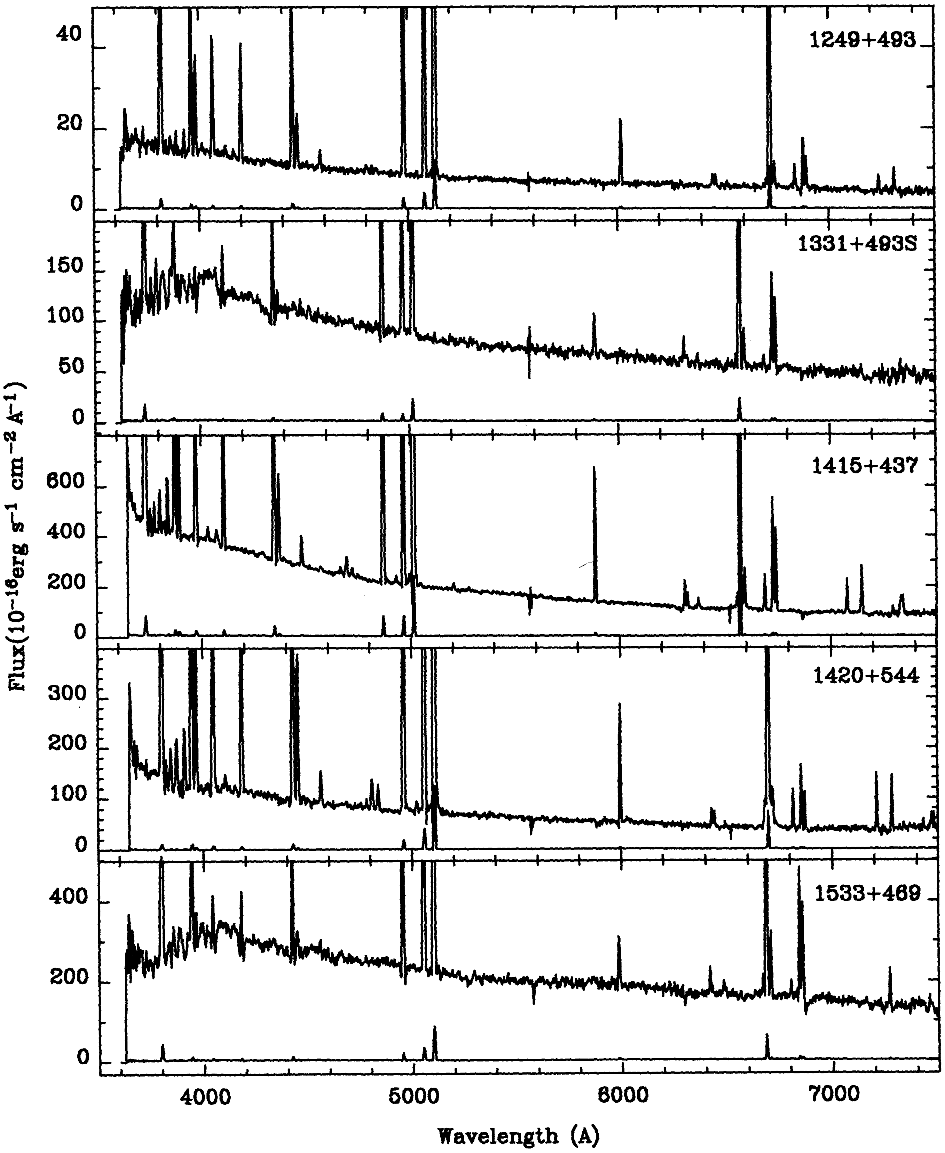

FIG. 1.—Mayall 4 m spectra of five galaxies in our blue compact galaxy sample. The spectra of 10 supergiant H II regions in the other nine BCGs can be found in Figs. 1 and 2 of Izotov, Thuan, & Lipovetsky (1994) (Paper I). Line identifications are also given in Fig. 1 of Paper I. Note the asymmetric low-intensity broad component of the Hβ λ4861, [O III] λ5007, and Hα λ6563 lines in 1420+544, indicative of fast gas motions.

inate, and a low-ionization zone with temperature T_e(O II), where O II, N II, S II, and Fe III lines originate. As for the Ar III and S III lines, they originate in both high- and low-ionization regions (Garnett 1992). The temperature T_e(O III) is calculated using the [O III] $\lambda4363/(\lambda4959+\lambda5007)$ ratio. To take into account the electron temperatures for different ions, we have used the results of the H II photoionization models of Stasinska (1990). We fit her models with the following expressions:

$$t_e(\text{O II}) = 0.243 + t_e(\text{O III})[1.031 - 0.184 t_e(\text{O III})] , \quad (1)$$

$$t_e(\text{Ne III}) = t_e(\text{O III}) , \quad (2)$$

$$t_e(\text{N II}) = t_e(\text{O II}) , \quad (3)$$

$$t_e(\text{S II}) = t_e(\text{O II}) , \quad (4)$$

$$t_e(\text{Fe III}) = t_e(\text{O II}) , \quad (5)$$

$$t_e(\text{He II}) = t_e(\text{O III}) , \quad (6)$$

where $t_e = T_e/10^4$ K.

Garnett (1992) has studied the behavior of T_e for different ions and has concluded that equations (2) and (3) are valid. He also examined the dependence of T_e(S III) and T_e(Ar III) on T_e(O III) and has derived the following relations which we adopt:

$$t_e(\text{Ar III}) = 0.83 t_e(\text{O III}) + 0.17 , \quad (7)$$

$$t_e(\text{S III}) = t_e(\text{Ar III}) . \quad (8)$$

For Ar IV, we adopt the relation from Stasinska (1993):

$$t_e(\text{Ar IV}) = t_e(\text{O III}) . \quad (9)$$

The [S II] $\lambda6717/\lambda6731$ ratio is used to determine the electron density N_e(S II), the minimum value of which was set to be 100 atoms cm^{-3}.

For ionic abundance determination, except for the case of Fe^{++}, we used the expressions from Pagel et al. (1992) with modifications for S III, where T_e(S III) was used instead of

© American Astronomical Society • Provided by the NASA Astrophysics Data System

1995ApJ...445..108T

TABLE 3

EMISSION-LINE INTENSITIES

Ion	1249+493		1331+493S		1415+437		1420+544		1533+469	
	F(λ)/F(Hβ)	I(λ)/I(Hβ)	F(λ)/F(Hβ)	I(λ)/I(Hβ)	F(λ)/F(Hβ)	I(λ)/I(Hβ)	F(λ)/F(Hβ)	I(λ)/I(Hβ)	F(λ)/F(Hβ)	I(λ)/I(Hβ)
3727 [O II]	0.943±0.037	1.070±0.044	2.387±0.062	2.355±0.064	1.018±0.014	1.060±0.015	0.535±0.015	0.558±0.016	2.492±0.057	2.249±0.062
3750 H12	0.012±0.005	0.043±0.019	...	...	0.016±0.002	0.048±0.008	0.017±0.003	0.020±0.004	...	...
3771 H11	0.029±0.006	0.062±0.013	...	...	0.021±0.002	0.053±0.006	0.039±0.004	0.043±0.005	...	...
3798 H10	0.032±0.006	0.064±0.012	...	...	0.031±0.002	0.063±0.005	0.056±0.004	0.060±0.005	...	...
3820 He I	...	...	...	...		0.262±0.005	0.575±0.013	0.595±0.014	...	...
3835 H9	0.035±0.006	0.067±0.011	...	...	...	...	...	...	...	...
3868 [Ne III]	0.367±0.017	0.408±0.020	0.280±0.015	0.276±0.016	...	...	...	...	0.413±0.017	0.372±0.018
3889 H8 + He I	0.173±0.012	0.219±0.015	0.027±0.010	0.047±0.018	0.160±0.004	0.193±0.005	0.190±0.007	0.199±0.008	0.088±0.009	0.239±0.032
3968 H7 + [Ne III]	0.237±0.013	0.287±0.017	0.048±0.009	0.067±0.014	0.228±0.004	0.262±0.005	0.331±0.009	0.343±0.010	0.097±0.009	0.263±0.031
4026 He I	0.017±0.003	0.018±0.004	...	...	0.016±0.001	0.017±0.001	0.014±0.002	0.014±0.002	...	...
4068 [S II]	0.013±0.003	0.014±0.004	0.036±0.007	0.034±0.007	0.018±0.001	0.019±0.001	0.003±0.001	0.003±0.001	...	...
4101 Hδ	0.217±0.012	0.258±0.015	0.107±0.009	0.125±0.012	0.263±0.005	0.294±0.005	0.274±0.008	0.284±0.008	0.119±0.009	0.270±0.025
4340 Hγ	0.436±0.017	0.476±0.019	0.363±0.012	0.374±0.014	0.422±0.005	0.448±0.006	0.476±0.010	0.486±0.011	0.367±0.013	0.470±0.020
4363 [O III]	0.101±0.007	0.106±0.008	0.046±0.007	0.045±0.007	0.085±0.002	0.086±0.002	0.169±0.006	0.172±0.006	0.087±0.007	0.077±0.007
4388 He I	0.006±0.002	0.006±0.002	...	...	0.002±0.001	0.002±0.001	0.005±0.001	0.005±0.001	...	...
4471 He I	0.034±0.004	0.035±0.004	0.020±0.005	0.020±0.005	0.030±0.001	0.030±0.001	0.037±0.003	0.037±0.003	0.032±0.005	0.029±0.006
4658 [Fe III]	...	...	...	...	0.009±0.001	0.009±0.001	0.003±0.001	0.003±0.001	...	...
4686 He II	0.015±0.003	0.015±0.003	...	...	0.023±0.001	0.023±0.001	0.007±0.001	0.007±0.001	0.011±0.005	0.010±0.005
4713 [Ar IV] + He I	0.008±0.002	0.008±0.002	...	...	0.012±0.001	0.012±0.001	0.034±0.002	0.034±0.002	0.005±0.004	0.004±0.004
4740 [Ar IV]	0.003±0.002	0.003±0.002	...	...	0.006±0.001	0.005±0.001	0.025±0.002	0.025±0.002	...	...
4861 Hβ	1.000±0.028	1.000±0.029	1.000±0.021	1.000±0.022	1.000±0.008	1.000±0.009	1.000±0.017	1.000±0.017	1.000±0.022	1.000±0.026
4922 He I	0.011±0.003	0.011±0.003	...	...	0.010±0.001	0.010±0.001	0.013±0.001	0.013±0.001	...	...
4959 [O III]	1.519±0.039	1.479±0.039	1.009±0.022	0.996±0.022	1.035±0.009	1.014±0.009	2.142±0.029	2.133±0.029	1.783±0.035	1.561±0.035
5007 [O III]	4.502±0.099	4.364±0.098	3.021±0.052	2.979±0.052	3.044±0.021	2.977±0.021	6.310±0.076	6.272±0.076	5.550±0.094	4.854±0.094
5199 [N I]	...	...	0.014±0.005	0.014±0.005	0.007±0.001	0.007±0.001	...	...	0.033±0.005	0.029±0.005
5518 [Cl III]	...	...	...	...	0.002±0.001	0.001±0.001	0.004±0.001	0.004±0.001	0.021±0.005	0.018±0.005
5538 [Cl III]	0.005±0.002	0.005±0.002	...	...	...	...	...	...	...	...
5755 [N II]	...	...	...	...	...	...	...	...	0.012±0.005	0.010±0.005
5876 He I	0.115±0.007	0.103±0.007	0.129±0.007	0.128±0.007	0.110±0.002	0.104±0.002	0.110±0.004	0.106±0.004	0.143±0.008	0.123±0.007
6300 [O I]	0.032±0.004	0.027±0.004	0.054±0.006	0.053±0.006	0.026±0.001	0.025±0.001	0.019±0.002	0.018±0.002	0.075±0.006	0.064±0.006
6312 [S III]	0.019±0.004	0.016±0.003	...	...	0.013±0.001	0.012±0.001	0.012±0.001	0.012±0.001	0.017±0.005	0.014±0.005
6363 [O I]	0.009±0.002	0.008±0.002	...	...	0.010±0.001	0.009±0.001	0.005±0.001	0.005±0.001	0.037±0.006	0.031±0.005
6563 Hα	3.283±0.076	2.783±0.071	2.846±0.050	2.815±0.054	2.968±0.020	2.756±0.021	2.893±0.038	2.761±0.040	3.204±0.059	2.812±0.064
6584 [N II]	0.039±0.005	0.033±0.004	0.104±0.007	0.102±0.007	0.035±0.001	0.033±0.001	0.019±0.003	0.018±0.003	0.180±0.009	0.154±0.009
6678 He I	0.035±0.005	0.030±0.004	0.030±0.006	0.030±0.006	0.029±0.001	0.027±0.001	0.031±0.002	0.029±0.002	0.048±0.006	0.041±0.006
6717 [S II]	0.096±0.007	0.080±0.006	0.276±0.011	0.273±0.011	0.094±0.002	0.086±0.002	0.052±0.003	0.049±0.003	0.353±0.013	0.300±0.013
6731 [S II]	0.053±0.006	0.044±0.005	0.194±0.009	0.192±0.009	0.070±0.002	0.064±0.002	0.026±0.002	0.025±0.002	0.259±0.011	0.220±0.011
7065 He I	0.029±0.005	0.024±0.004	...	...	0.027±0.001	0.025±0.001	0.049±0.003	0.046±0.003	...	...
7136 [Ar III]	0.041±0.006	0.033±0.005	...	...	0.042±0.002	0.039±0.002	0.047±0.003	0.044±0.003	0.101±0.009	0.085±0.009
7281 He I	...	...	...	...	0.006±0.001	0.006±0.001	0.005±0.002	0.005±0.002	...	...
7320 [O II]	...	...	0.034±0.008	0.034±0.008	0.027±0.002	0.024±0.002	0.016±0.003	0.015±0.002	...	...
7330 [O II]	...	...	...	...	0.025±0.001	0.023±0.001	0.011±0.002	0.010±0.002	...	...
C(Hβ) mag	0.200		0.000		0.080		0.060		0.040	
F(Hβ)(×10^{14}) ergs s^{-1}cm^{-2}Å^{-1}	0.2		0.5		6.9		1.7		1.4	
EW(Hβ) Å	120		28		150		231		30	
EW(abs) Å	1.9		0.4		2.4		0.3		4.2	

© American Astronomical Society • Provided by the NASA Astrophysics Data System

1995ApJ...445..108T

T_e(O III). For Fe^{++}, using emissivities by Garstang, Robb, & Rountree (1978) we have derived

$$\frac{N(\mathrm{Fe}^{++})}{N(\mathrm{H}^+)} = 2.3 \times 10^{-6} E^0_{4,2} \sqrt{t}\, 10^{1.34/t} \frac{I(\lambda 4658)}{I(\mathrm{H}\beta)}, \quad (10)$$

where

$$E^0_{4,2} = 1.387 t^{-0.983}\, 10^{-0.0424/t} \quad (11)$$

and $t = t_e$(Fe III).

To obtain the total abundances of elements, it is necessary to take into account unseen stages of ionization. Then the total abundance of element A is equal to

$$\frac{\mathrm{A}}{\mathrm{H}} = \mathrm{ICF(A)} \frac{\mathrm{A}^{+i}}{\mathrm{H}^+}, \quad (12)$$

where ICF(A) is the ionization correction factor for element A.

For oxygen, we adopted the following expression for the total abundance

$$\frac{\mathrm{O}}{\mathrm{H}} = \frac{\mathrm{O}^+ + \mathrm{O}^{++}}{\mathrm{H}^+}. \quad (13)$$

In seven of our galaxies, the nebular He II λ4686 line was detected. Therefore part of the oxygen in those BCGs is in the O^{+3} stage. However, the weakness of the He II λ4686 line means that the ionic abundance of O^{+3} does not exceed 2%–3% of the total oxygen abundance (Skillman & Kennicutt 1993). Therefore we do not take the O^{+3} ionic abundance into consideration.

For nitrogen and neon, we have used the following common expressions for the correction factors:

$$\mathrm{ICF(N)} = \frac{\mathrm{O}}{\mathrm{O}^+}, \quad (14)$$

$$\mathrm{ICF(Ne)} = \frac{\mathrm{O}}{\mathrm{O}^{++}}. \quad (15)$$

Garnett (1990) has studied the nitrogen ionic composition of giant H II regions. In low-excitation H II regions the correction factor is shown to be a sensitive function of the adopted stellar atmosphere models of ionizing stars. However in nebulae having low abundances and/or ionizing stars hotter than 40,000 K, the N^+/O^+ is an accurate estimate of N/O. For these H II regions, Garnett (1990) using photoionization model calculations has obtained numerical coefficients ranging from 0.8 to 1.0 in equation (14). In order to compare our results with other data, we have set the coefficient to be 1.0 in equation (14).

Using Stasinska (1990)'s photoionization H II models, we have derived the following expression for the ionization correction factor of Fe:

$$\mathrm{ICF(Fe)} = \frac{\mathrm{Fe}}{\mathrm{Fe}^{++}} = 1.25 \frac{\mathrm{O}}{\mathrm{O}^+}. \quad (16)$$

Correction factors for Ar and S are more complex since Ar^{++} and S^{++} exist in both O^{++} and O^+ zones. Garnett (1989) has studied the dependence of the correction factor for sulfur on the O^+/O ratio for different LTE and non-LTE stellar atmospheres models of ionizing stars and found that the difference is very small for stars with effective temperatures $T_{\mathrm{eff}} \geq 40{,}000$ K. Only in low-excitation H II regions, which is not the case here, is ICF(S) strongly dependent on the metallicity of the ionizing stars. We assume that S^{+3} and Ar^{+3} follow the same behavior as these two ions coexist in high-excitation H II regions. Using the results of model calculations of photoionized H II regions by Stasinska (1990), we obtained the following analytic approximations for ICF(S) and ICF(Ar):

$$\mathrm{ICF(S)} = \frac{\mathrm{S}}{\mathrm{S}^+ + \mathrm{S}^{++}} = [\![0.013 + x\{5.10 + x[-12.78 + x(14.77 - 6.11x)]\}]\!]^{-1}, \quad (17)$$

$$\mathrm{ICF(Ar)} = \frac{\mathrm{Ar}}{\mathrm{Ar}^{++} + \mathrm{Ar}^{+++}} = \{0.99 + x[0.091 + x(-1.14 + 0.077x)]\}^{-1}, \quad (18)$$

$$\mathrm{ICF(Ar)} = \frac{\mathrm{Ar}}{\mathrm{Ar}^{++}} = [0.15 + x(2.39 - 2.64x)]^{-1}, \quad (19)$$

where $x = O^+/O$. In galaxies where the [Ar IV] λ4740 emission line is not seen, equation (19) has been used instead of equation (18).

The ionic and total heavy element abundances along with the adopted ICFs for the five H II regions for which spectra are shown in Figure 1 are given in Table 4. The corresponding results for the 10 other H II regions can be found in Paper I. We summarize in Table 5 our abundance results for the total sample. We give for each of the 15 H II regions the oxygen abundance and the abundances of nitrogen, neon, sulfur, and argon relative to oxygen. We also give iron abundances for seven BCGs, the data for the other seven galaxies being not good enough to permit an accurate iron abundance determination. We emphasize that, because of their high signal-to-noise ratio, our spectra show, besides the iron lines, many other weak lines seldom seen before in published BCG spectra. Thus, emission lines of ions with different degrees of ionization of elements such as oxygen, sulfur, and argon can be seen, allowing for more accurate ionization correction factors and for more precise total abundance determinations.

Table 5 gives also the uncertainties in the derived abundances. These include the uncertainties in the line flux measurements due to spectral noise and continuum placement. They are small (≲5%) because of the high signal-to-noise ratio of our spectra. In a few galaxies, the [Fe III] λ4658 and He II λ4686 lines are blended with broad Wolf-Rayet features, and the [N II] λ6584 line is affected by the broad low-intensity broad wings of the Hα λ6563 line (Thuan et al. 1994). The Wolf-Rayet and broad wings were Gaussian fitted and removed before the line measurements. The uncertainties in Table 5 also take into account errors in the determination of the electron temperature T_e(O III), one of the major sources of uncertainties because of the exponential temperature dependence of ionic abundances derived from collisionally excited forbidden lines. Since T_e(O III) is determined from the [O III] (λ4959 + λ5007)/λ4363 line intensity ratio, and the λ4959 and λ5007 lines are the strongest ones in the spectra, most of the uncertainty in T_e(O III) comes from the continuum placing for the λ4363 line. Since the H II regions in our BCG sample are of high excitation, typical relative errors in the [O III] λ4363 flux do not exceed 5%, leading to errors of the same order in T_e and errors smaller than 10% in the ionic abundances. The good agreement between the Balmer line ratios, after correc-

© American Astronomical Society • Provided by the NASA Astrophysics Data System

1995ApJ...445..108T

TABLE 4

IONIC AND TOTAL HEAVY ELEMENT ABUNDANCES

Property	Galaxy				
	1249+493	1331+493S	1415+437	1420+544	1533+469
T_e(OIII)(K)	15,900	13,000	17,400	16,900	13,300
T_e(OII)(K)	14,200	12,700	14,800	14,600	12,900
T_e(SIII)(K)	14,900	12,500	16,100	15,700	12,800
N_e(SII)(cm^{-3})	100	100	100	100	100
$O^+/H^+(\times 10^4)$	0.11±0.01	0.35±0.06	0.10±0.00	0.05±0.00	0.32±0.04
$O^{+2}/H^+(\times 10^4)$	0.41±0.04	0.47±0.08	0.23±0.01	0.52±0.02	0.71±0.08
$O/H(\times 10^4)$	0.52±0.04	0.82±0.10	0.33±0.01	0.57±0.03	1.03±0.08
12+log(O/H)	7.72±0.03	7.91±0.05	7.51±0.01	7.75±0.02	8.01±0.04
$N^+/H^+(\times 10^6)$	0.27±0.03	1.05±0.18	0.25±0.01	0.14±0.01	1.54±0.17
ICF	4.72	2.35	3.39	10.75	3.24
$N/H(\times 10^6)$	1.30±0.22	2.48±0.65	0.84±0.05	1.53±0.14	4.99±0.87
12+log(N/H)	6.11±0.07	6.39±0.11	5.92±0.03	6.18±0.04	6.70±0.08
$Ne^{++}/H^+(\times 10^5)$	0.84±0.09	1.04±0.18	0.43±0.02	1.04±0.06	1.30±0.15
ICF	1.27	1.74	1.42	1.10	1.45
$Ne/H(\times 10^5)$	1.07±0.14	1.81±0.38	0.61±0.03	1.15±0.08	1.88±0.27
12+log(Ne/H)	7.03±0.06	7.26±0.09	6.78±0.02	7.06±0.03	7.27±0.06
$S^+/H^+(\times 10^6)$	0.14±0.03	0.62±0.07	0.15±0.01	0.08±0.02	0.68±0.06
$S^{++}/H^+(\times 10^6)$	0.84±0.17	...	0.48±0.04	0.51±0.06	1.24±0.42
ICF	1.54	...	1.35	2.58	1.34
$S/H(\times 10^6)$	1.51±0.22	...	0.86±0.04	1.51±0.11	2.57±0.48
12+log(S/H)	6.18±0.06	...	5.93±0.02	6.18±0.03	6.41±0.08
$Ar^{++}/H^+(\times 10^7)$	1.21±0.17	...	1.24±0.05	1.46±0.11	4.12±0.42
$Ar^{+++}/H^+(\times 10^7)$	0.40±0.27	...	0.57±0.07	2.72±0.23	...
ICF	1.85	...	1.08	1.01	1.57
$Ar/H(\times 10^7)$	2.23±0.24	...	1.95±0.09	4.21±0.26	6.45±0.53
12+log(Ar/H)	5.35±0.05	...	5.29±0.02	5.62±0.03	5.81±0.04
Fe^{++}/H^+ $(\times 10^6)$	...	...	0.18±0.02	0.06±0.02	...
ICF	...	...	4.23	13.44	...
Fe/H $(\times 10^6)$	...	...	0.78±0.03	0.77±0.07	...
12+log(Fe/H)	...	...	5.89±0.02	5.89±0.04	...

TABLE 5

HEAVY ELEMENT ABUNDANCE RATIOS

Galaxy	12+log(O/H)	log(N/O)	log(Ne/O)	log(S/O)	log(Ar/O)	log(Fe/O)
0832+699	7.58±0.02	−1.67±0.05	−0.73±0.05	−1.57±0.05	−2.26±0.04	...
0940+544N	7.37±0.02	−1.56±0.07	−0.67±0.06	−1.54±0.06	−2.15±0.06	−1.70±0.06
0946+558	8.04±0.01	−1.52±0.04	−0.69±0.03	−1.45±0.03	−2.33±0.03	..
0948+532	8.04±0.02	−1.46±0.06	−0.69±0.04	−1.50±0.05	−2.14±0.04	−1.88±0.05
1135+581	8.02±0.01	−1.47±0.03	−0.64±0.03	−1.56±0.03	−2.23±0.02	−1.69±0.02
1152+579	7.85±0.01	−1.46±0.03	−0.70±0.03	−1.56±0.03	−2.28±0.03	−1.70±0.03
1159+545	7.47±0.02	−1.55±0.07	−0.70±0.06	−1.53±0.06	−2.18±0.06	−1.74±0.07
1211+540	7.68±0.01	−1.60±0.04	−0.74±0.03	−1.46±0.03	−2.21±0.03	...
1249+493	7.72±0.03	−1.61±0.08	−0.69±0.07	−1.54±0.07	−2.37±0.06	...
1331+493N	7.82±0.01	−1.56±0.04	−0.70±0.03	−1.52±0.04	−2.32±0.03	...
1331+493S	7.91±0.05	−1.52±0.13	−0.66±0.11	...	...	...
1415+437	7.51±0.01	−1.59±0.03	−0.73±0.02	−1.58±0.02	−2.22±0.02	−1.62±0.02
1420+544	7.75±0.02	−1.57±0.04	−0.70±0.04	−1.57±0.04	−2.13±0.03	−1.87±0.04
1437+370	7.97±0.02	−1.52±0.06	−0.68±0.05	−1.52±0.05	−2.19±0.04	...
1533+469	8.01±0.04	−1.31±0.08	−0.74±0.07	−1.60±0.09	−2.20±0.05	...
Weighted mean	...	−1.53±0.08	−0.70±0.03	−1.54±0.04	−2.23±0.07	−1.74±0.10

© American Astronomical Society • Provided by the NASA Astrophysics Data System

1995ApJ...445..108T

tion for extinction and underlying stellar absorption, with the theoretical values gives us confidence that these two corrections were done correctly and in a self-consistent manner, introducing uncertainties not more than 10%. Other uncertainties, not included in the quoted error bars and more difficult to evaluate, are related to the atomic data (recombination coefficients, ionization, and excitation cross sections). The dielectronic recombination coefficients for some complex ions, such as iron ions, may be uncertain but are unlikely to change the abundances by more than 50%.

3.2. *Oxygen*

As can be seen from Table 5, our BCG sample contains many low-metallicity galaxies, most of which were found in the Second Byurakan survey (SBS). The high fraction of metal-deficient BCGs in the SBS has been pointed out by Izotov et al. (1990a, b, 1991, 1992a, b) on the basis of low signal-to-noise ratio Russian 6 m telescope spectra. The present work, while confirming the early findings, gives more precise abundances, thanks to high signal-to-noise ratio spectra. Hereafter, we shall denote the abundance of element A relative to that of hydrogen by $N(\mathrm{A}) \equiv 12 + \log(\mathrm{A/H})$. Two galaxies in our sample, 0940+544N and 1159+545, have respectively an oxygen abundance as low as 1/35 and 1/29 that of the Sun [$N(\mathrm{O})_\odot = 8.91$; Anders & Grevesse 1989, Meyer 1989). These oxygen abundances are very close to those in the most metal-deficient BCGs known, I Zw 18 ($Z_\odot/50$) (Searle & Sargent 1972) and SBS 0335−052 ($Z_\odot/41$) (Izotov et al. 1990a, b; Melnick, Heydary-Malayeri, & Leysi 1992). Six galaxies in our sample (the two mentioned above plus 0832+699, 1211+540, 1249+493, and 1415+437) have oxygen abundances less than 1/15 of the solar value, while the remaining eight have oxygen abundances between 1/15 and one-seventh of the solar value. The number of known BCGs with very low metallicity, say less than $Z_\odot/15$, is very small. Besides I Zw 18 and SBS 0335−052, there were Tol 65 ($Z_\odot/22$) and T1214−277 ($Z_\odot/21$) (Pagel et al. 1992). We have more than doubled the low-metallicity sample in this work, a sample which will allow us to study heavy element abundances in a very metal deficient environment.

3.3. *Nitrogen*

In Figure 2, we show the dependence of the nitrogen-to-oxygen abundance ratio as a function of oxygen abundance for our BCG sample (*filled circles*). We have also shown the data from Garnett (1990) for a different sample of 33 BCGs and dwarf irregular galaxies (*asterisks*) and from Skillman & Kennicutt (1993) for I Zw 18 (*filled triangle*). The open circles show the data for H II regions in the nearby spiral galaxy M101 (Torres-Peimbert et al. 1989), and the solid line is the fit for solar neighborhood dwarf stars from Tomkin & Lambert (1984). Our BCG data show two striking features: (1) N/O is constant and independent of O/H; (2) N/O shows an extraordinarily small dispersion. The weighted mean value of log N/O for our eight metal-deficient BCGs [$7.37 \leq N(\mathrm{O}) \leq 7.82$] is −1.58 with a dispersion of only ±0.02, while the weighted mean value for the whole sample is $\langle \log \mathrm{N/O} \rangle = -1.53 \pm 0.08$. This is to be compared with the weighted mean

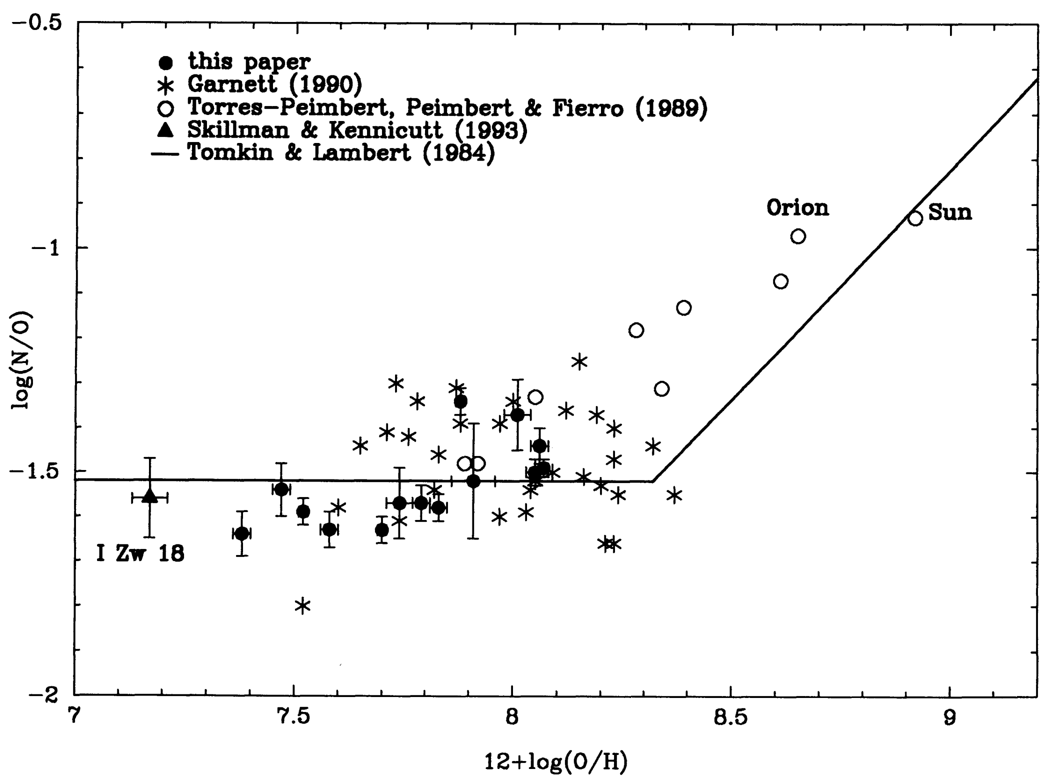

FIG. 2.—Nitrogen-to-oxygen abundance ratio as a function of oxygen abundance. Our BCG sample is shown in filled circles. For comparison, the data for I Zw 18 (*filled triangle*; Skillman & Kennicutt 1993), the irregular galaxy and BCG sample of Garnett (1990, *asterisks*), H II regions in M101, Orion, and the Sun (*open circles*; Torres-Peimbert, Peimbert, & Fierro 1989) are also shown. The solid line represents the mean trend for galactic dwarf stars (Tomkin & Lambert 1984). Note the absence of correlation between log N/O and $N(\mathrm{O}) \equiv 12 + \log \mathrm{O/H}$ and the small dispersion of the BCG data points.

© American Astronomical Society • Provided by the NASA Astrophysics Data System

1995ApJ...445..108T

$\langle \log \mathrm{N/O} \rangle = -1.49 \pm 0.15$ for Garnett's data in the range $7.37 \leq N(\mathrm{O}) \leq 7.82$, and $\langle \log (\mathrm{N/O}) \rangle = -1.46^{+0.10}_{-0.13}$ for the whole sample. There are two comments to be made. First, while $\langle \log \mathrm{N/O} \rangle$ for our eight most metal-deficient BCGs is similar to the mean value of -1.58 ± 0.05 obtained by Skillman & Kennicutt (1993) for the NW and SE components in I Zw 18, it is lower than the mean value for Garnett's data in the same metallicity range. It is evident from Figure 2 that our data points lie at the lower envelope of Garnett's data. Second, the dispersion about the mean of our data is much smaller than that shown by Garnett's data set. There are at least two reasons for the larger scatter. First, Garnett's data, being collected from a variety of different authors using different instruments and methods of analysis, are by nature heterogeneous and would show a larger dispersion than our homogeneous data set. Second, the N/O ratio depends sensitively on the ionization correction factor ICF(N) = $\mathrm{O/O^+}$. By obtaining the whole spectral range in a single exposure, we can achieve good internal precision in the derivation of extinction coefficients and get reliable intensities for the reasonably strong [O II] λ3727 line. Instead, Garnett (1990) used the weaker and more uncertain near-infrared emission lines [O II] $\lambda\lambda$7319, 7331.

As for our generally lower N/O ratios, we suspect that this may be due to the contamination of the weak [N II] $\lambda\lambda$6548, 6584 lines by broad wings of Hα λ6563 in the low-resolution data used by Garnett (1990). These broad wings may be instrumental (Garnett 1990) or, as discussed before, real and caused by fast gas motions (Δv = 2000–4000 km $\mathrm{s^{-1}}$) powered by supernova explosions. Because of the low intensity of these broad Hα components (1%–2% of peak intensity), high signal-to-noise ratio spectra with a resonably high spectral resolution ($\leq$7 Å) are needed to detect them and remove their contribution to the N II lines. A case in point is that of I Zw 18. Dufour, Garnett, & Shields (1988) obtained for this galaxy log N/O = -1.25 ± 0.18, while Garnett (1990) derived log N/O = -1.36 ± 0.18. Skillman & Kennicutt (1993) using high signal-to-noise ratio high spectral resolution spectra found a broad low-intensity Hα component and substracted it from the N II lines to obtain lower log N/O values: -1.56 ± 0.09 for the NW component and -1.60 ± 0.06 for the SE component.

For the five BCGs in our sample which exhibit a low-intensity broad Hα component (0940+544N, 1135+581, 1152+579, 1415+437, and 1420+544), we have fitted a Gaussian profile to the broad component and removed it from the [N II] lines. The most spectacular case of contamination is that for 1420+544: subtracting the broad Hα component leads to a decrease of its [N II] λ6584 line intensity by a factor of 2.

The constancy of log N/O as a function of log O/H for BCGs with $7.1 \leq N(\mathrm{O}) \leq 8.3$ implies that N is mainly primary in origin in low-metallicity BCGs, a conclusion reached before by many authors (Vila-Costas & Edmunds 1993 and references therein). The new contribution of this work is the result that the dispersion about the mean of log N/O is remarkably small. Furthermore, the scatter in N/O does not grow as O/H decreases. The small dispersion puts very severe constraints on time-delay models. Because O is thought to be made in massive ($M > 9\ M_\odot$) stars, while primary N is thought to be made in intermediate-mass ($4\ M_\odot \leq M \leq 9\ M_\odot$) stars by carbon dredge-up (Renzini & Voli 1981), there is necessarily a time delay between the injection of O and N in the ISM because of the different evolutionary timescales of stars with different masses. This time delay, which can be as large as 5×10^8 yr, introduces a significant ($\geq \pm 0.2$) scatter in log N/O, as galactic evolution models by Marconi et al. (1994) and Pilyugin (1993) show. Furthermore, these models also predict an increase in the scatter of log N/O toward lower metallicities, as the relative contamination by N and O is more important for more pristine gas. Both of these predictions by time-delay models are contrary to the trends of the observations presented here. Thus, if we take the observations presented in Figure 2 at face value, there must not be a significant time delay between O and primary N production, i.e., that these two elements must be made in the same massive ($M \geq 10\ M_\odot$) stars.

Conventional nucleosynthesis models do not allow for such a possibility. However, metal-poor massive stars ($M \geq 30\ M_\odot$) can produce primary nitrogen if the numerical parameters governing convective overshoot are enlarged (Timmes 1994). The synthesis of primary nitrogen occurs as the convective helium-burning shell penetrates into the hydrogen shell with violent, almost explosive, consequences. The amount of convective overshoot necessary to produce primary nitrogen is within the uncertainties of convection theory. However, the exact amount of nitrogen ejected is not well determined as it depends on the zoning employed and the treatment of convection (Timmes 1994). Woosley & Weaver (1982) have studied the evolution of a 500 $M_\odot$, zero-metallicity Population III star and found in their model that a small density gradient allows carbon-rich material from the core to be mixed up in the hydrogen-burning shell, where N is produced by the CN cycle. Ultimately, the outer envelope, containing mostly N and He, may be lost by a stellar wind, while the core collapses to a black hole. Again, the exact amount of N made depends on poorly known overshooting parameters. The sensitivity of the amount of primary nitrogen produced in stellar models means that observations of nitrogen abundances in BCGs may be an excellent discriminant of various treatments of convection (Timmes 1994).

If O and primary N are both made in the same massive stars, this implies that the latter is *not* made abundantly in the intermediate-mass stars. This may be due perhaps to a large lower mass cutoff of the initial mass function ($M_l \sim 10\ M_\odot$) so that intermediate-mass stars do not exist and/or a low mixing length in the convective zone of these stars which prevents the dredged-up carbon-rich material from reaching the hydrogen-burning shell.

Beyond $N(\mathrm{O}) \sim 8$ ($Z \sim Z_\odot/8$), the dispersion increases to ± 0.08, accompanied by a rise in the mean log N/O which becomes -1.46. A straightforward interpretation of this behavior is that while primary N production predominates in BCGs with $N(\mathrm{O}) \leq 8$, secondary N production becomes more important at higher metallicities. This interpretation is supported by the data of Torres-Peimbert et al. (1989) on H II regions in the nearby spiral M101 which show a roughly linear increase of log N/O beyond $N(\mathrm{O}) \sim 8$, a relationship predicted by the simple model of galactic evolution with the instantaneous recycling approximation, if N is a secondary element. Our BCG sample does not contain enough high-metallicity galaxies to define precisely the O/H abundance where N switches from being mainly primary to being mainly secondary. The data for solar neighborhood galactic G dwarf stars of Tomkin & Lambert (1984) (Fig. 2, *solid line*) suggest the transition occurs at $N(\mathrm{O}) \sim 8.3$, a conclusion supported by the galaxy data of Shields, Skillman, & Kennicutt (1991).

3.4. *Neon, Sulfur, and Argon*

The elements neon, sulfur, and argon are all products of α-processes during both hydrostatic burning and explosive

© American Astronomical Society • Provided by the NASA Astrophysics Data System

1995ApJ...445..108T

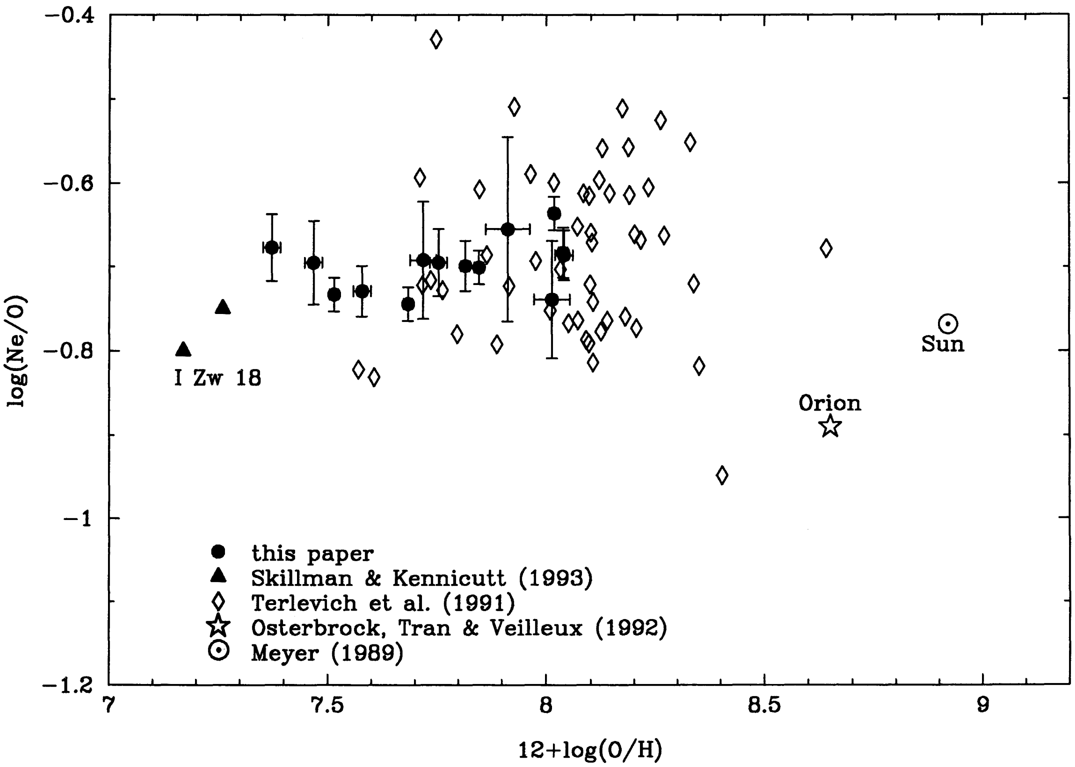

FIG. 3.—Neon-to-oxygen abundance ratio as a function of oxygen abundance. Our BCG sample is shown in filled circles. Also plotted for comparison are the data for I Zw 18 for both its NW and SE components (*filled triangles*; Skillman & Kennicutt 1993) and for H II galaxies from the catalog of Terlevich et al. (1991) (*open diamonds*). The Orion point is from Osterbrock, Tran, & Veilleux (1992) and that of the Sun is from Meyer (1989). Note the absence of correlation between log Ne/O and N(O) for $N(\mathrm{O}) \leq 8.0$ and the small dispersion of log Ne/O for our BCG sample.

nucleosynthesis in massive stars. Their abundances relative to oxygen for the BCGs in our sample are given in Table 5.

We show in Figure 3 the dependence of log Ne/O on oxygen abundance for our BCG sample (*filled circles*). As expected for a α-process element, Ne/O is constant and independent of O/H. We note again the very small dispersion about the mean of the ratio: $\langle \log \mathrm{Ne/O} \rangle = -0.70 \pm 0.03$. We have compared our results with those for other BCG samples. We have shown in Figure 3 the data of Skillman & Kennicutt (1993) for both the NW (log Ne/O = -0.80) and SE (log Ne/O = -0.75) components of I Zw 18 (*filled triangles*). We have also shown the data of Terlevich et al. (1991) for H II galaxies in the southern hemisphere (*open diamonds*). The neon and oxygen abundances have been calculated using the emission-line intensities given by those authors in their spectrophotometric catalog. It is evident that, while the means are similar, our data show a smaller dispersion. The sample of Terlevich et al. has $\langle \log \mathrm{Ne/O} \rangle = -0.68 \pm 0.10$. Examination of other BCG samples also reveals a larger dispersion than ours. For the sample of Vigroux et al. (1987) who compiled BCG data from the literature, $\langle \log \mathrm{Ne/O} \rangle = -0.67 \pm 0.10$, while for the BCGs in the Calán-Tololo survey of Peña, Ruiz, & Maza (1991), $\langle \log \mathrm{Ne/O} \rangle = -0.67 \pm 0.12$. We can think of several reasons which may explain the higher dispersion in other data sets. First, other data sets are more heterogeneous, coming from different authors or obtained with different telescopes, while our data were obtained in the same run at the same telescope. Second, and more importantly, thanks to our high signal-to-noise ratio data, we have corrected the spectra for extinction and underlying stellar absorption to obtain the theoretical Balmer decrements, using all available hydrogen lines in the Balmer series, from Hα λ6563 to H12 λ3750. Instead, Peña et al. (1991) used only three lines (Hα, Hβ, and Hγ) to correct for extinction. Therefore, some of their BCGs have Hδ λ4102, H8 + He I λ3889, and H9 λ3835 line intensities which quite differ from their theoretical values. Since the [Ne III] λ3868 emission line which plays a key role in the neon abundance determination lie near these lines, it is also in all likelihood, incorrectly corrected for extinction. The same effect appears to be present in the results on I Zw 18 of Skillman & Kennicutt (1993). Because the intensity of the H8 + He I λ3889 emission line is $\sim$15% lower than the theoretical value, we suspect that the blue part of the spectrum of I Zw 18 is under-corrected for extinction, leading to an underestimation of the I Zw 18 Ne abundance, which is $\sim$15% lower than the mean value for our sample. Terlevich et al. (1991) have also noted that their observations may suffer from nonlinearity effects of the image dissector scanner (IDS) they used and from second-order contamination near Hα λ6563. We thus believe that the larger dispersions in the previous BCG samples are not real but due to observational uncertainties.

We have also plotted in Figure 3 the data for the Orion Nebula (Osterbrock, Tran, & Veilleux 1992) and for the Sun (Meyer 1989). Both the Orion (log Ne/O = -0.89) and solar (log Ne/O = -0.77) values are lower than the mean value of our BCG sample, but they are also more uncertain. Orion, which is a low-ionization H II region, has a more uncertain ionization correction factor (Torres-Peimbert et al. 1989), while the determination of Ne in the Sun is notoriously difficult (Meyer 1989).

© American Astronomical Society • Provided by the NASA Astrophysics Data System

1995ApJ...445..108T

The dependence of the S/O ratio on O/H for our BCG sample is shown by filled circles in Figure 4. For comparison, we have also shown the data of Garnett (1989) for a sample of 13 BCGs and dwarf irregulars (*open circles*) and that of Torres-Peimbert et al. (1989) for H II regions in the spiral galaxy M101 (*crosses*) and for Orion and the Sun. The data for I Zw 18 from Skillman & Kennicutt (1993) is also shown as a square. The NW and SE clumps in this galaxy have nearly the same log S/O, so we take the mean $\langle \log \text{S/O} \rangle = -1.70$. Examination of Figure 4 shows that our data points lie systematically higher than those from other authors. To understand this systematic shift, let us recall that in the type of galaxies studied here, sulfur is mostly in the S^{++} form (see Table 4). To derive sulfur abundances, it is therefore quite important to detect [S III] emission lines. Garnett (1989) used the nebular [S III] $\lambda\lambda$9069, 9531 emission lines in the near-infrared, while we used the auroral [S III] λ6312 line. To correct for unseen sulfur ionization stages, we have used the ionization correction factor given by equation (17). Instead of setting T_e(S III) = T_e(O III) as done by Garnett (1989) and Torres-Peimbert et al. (1989), we use T_e(S III) as calculated by equations (7) and (8) which give values generally lower than T_e(O III) (see Table 4). This is because the S^{++} ionization zone overlaps with both the O^+ and O^{++} zones, so that T_e(S III) is intermediate between T_e(O II) and T_e(O III). The systematically higher temperatures T_e(S III) adopted by other authors lead to systematically lower S/O ratios. If we were to correct the data of Garnett (1989) and Torres-Peimbert et al. (1989) by the temperature differences, their data would agree quite well with ours whose mean value $\langle \log \text{S/O} \rangle$ is -1.54 ± 0.04. To illustrate the effect of the temperature differences, we have shown by an arrow in Figure 4 how the I Zw 18 point would move upward (by $\Delta \log$ S/O ~ 0.1) if T_e(S III) from Garnett (1992) is used instead of T_e(S III) = T_e(O III). While the dispersion about the mean of log S/O for our data set is similar to that for Torres-Peimbert et al. (1989) (± 0.03), it is smaller than that for Garnett (1989) (± 0.12). Again, we attribute our smaller dispersion to higher signal-to-noise ratio data and to a higher internal consistency.

Taking into account the systematic shift of the other data sets, Figure 4 shows that S/O is constant and independent of O/H. This is as expected since S is an α-process element produced in the same massive stars as O.

To derive the abundance of argon, we use the [Ar IV] λ4740 and [Ar III] λ7135 emission lines which probe two different ionization stages. T_e(Ar III) and T_e(Ar IV) are given by equations (7) and (9). As for S^{++}, the ionization zone of Ar^{++} is intermediate between the O^+ and O^{++} zones. To correct for unseen ionization stages, we have used equations (18) and (19).

In Figure 5, we have shown the run of log Ar/O versus oxygen abundance for our BCG sample (*filled circles*) along with data for other H II regions in M101, Orion and the Sun (*crosses*; Torres-Peimbert et al. 1989) and for the BCGs I Zw 18 and II Zw 40 (*open circles*; Stevenson et al. 1993). The agreement between the different data sets is good, with the exception of I Zw 18 which has a lower Ar/O. The reason for this lower value is not clear. As is the case for Ne/O and S/O, Ar/O shows no dependence on O/H. Like other α-elements, Ar is made in the same massive stars as O. The weighted mean

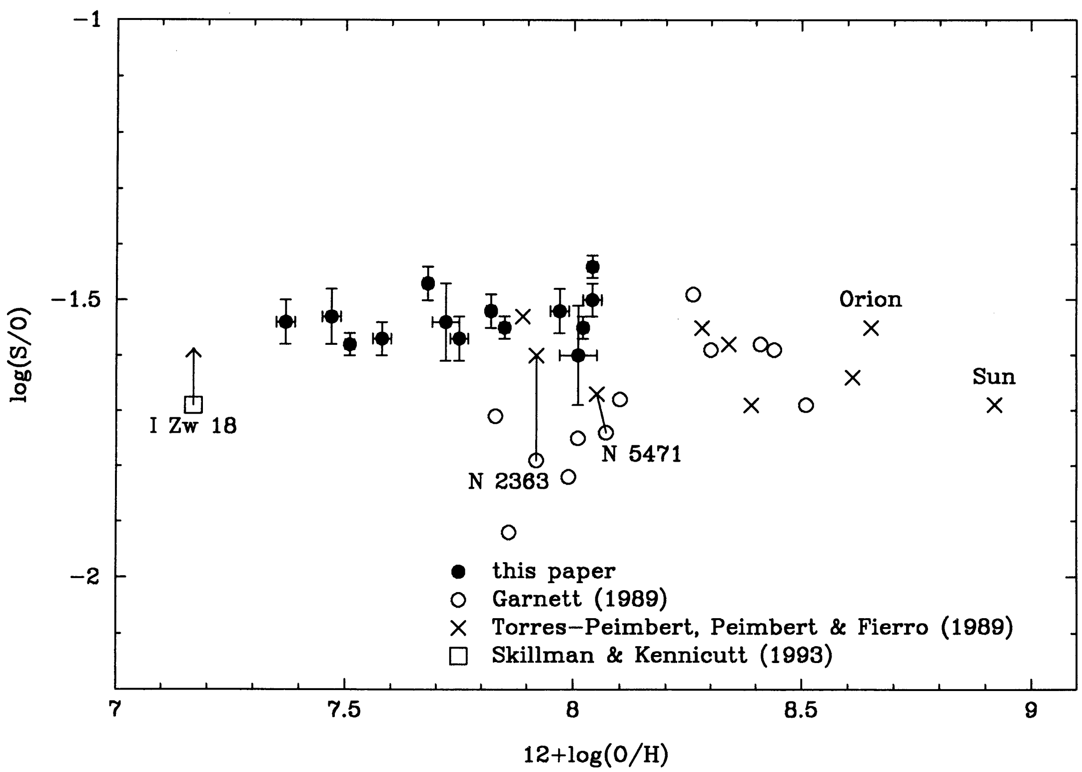

FIG. 4.—Sulfur-to-oxygen abundance ratio as a function of oxygen abundance. Our BCG sample is shown in filled circles. For comparison, the data for H II regions in the spiral galaxy M101, Orion, and the Sun (*crosses*; Torres-Peimbert, Peimbert, & Fierro 1989), for the BCG and dwarf irregular galaxy sample of Garnett (1989; *open circles*), and for I Zw 18 of Skillman & Kennicutt (1993; *open square*) are also shown. Different observations of the same objects are connected by solid lines. The arrow shows how the I Zw 18 data point would move upward if the electron temperature T_e(S III) instead of T_e(O III) is used to derive the S^{++} abundance. Note again the absence of correlation between log S/O and N(O) and the small dispersion of the S/O ratio for our BCG sample.

© American Astronomical Society • Provided by the NASA Astrophysics Data System

1995ApJ...445..108T

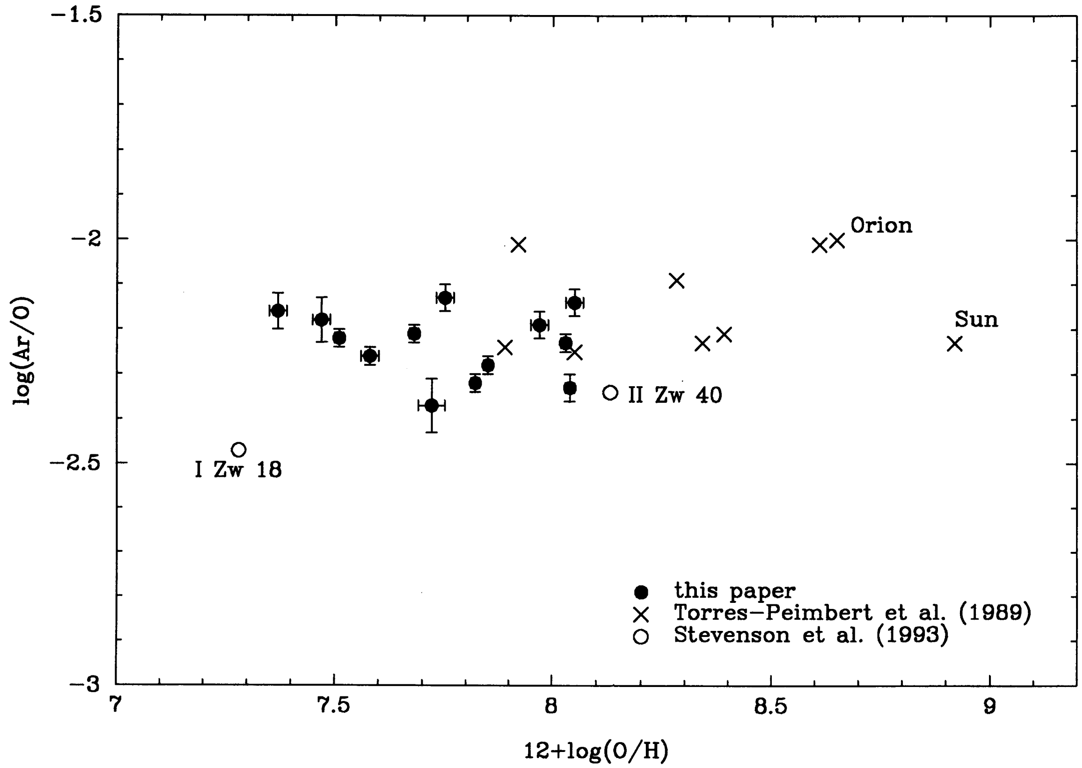

FIG. 5.—Argon-to-oxygen abundance ratio as a function of oxygen abundance. Our BCG sample is shown in filled circles. For comparison, the data for the two BCGs I Zw 18 and II Zw 40 (*open circles*; Stevenson, McCall, & Welch 1993) and for H II regions in dwarf and spiral galaxies and for Orion and the Sun (*crosses*; Torres-Peimbert, Peimbert, & Fierro 1989) are also shown. There is no correlation between log Ar/O and N(O).

$\langle \log \mathrm{Ar/O} \rangle$ for our sample is 2.23 ± 0.07. We also obtain $\langle \log \mathrm{Ar/S} \rangle = -0.69$, in good agreement with the value obtained by Stevenson et al. (1993) for their H II region sample.

To summarize, the abundance relative to oxygen of all three α-elements Ne, S, and Ar shows no dependence on O/H, confirming that they are all made in the same massive stars as oxygen, and that their production does not depend on the stellar initial chemical composition. All these elements are manufactured mainly during hydrostatic burning, although some S and Ar can be produced during explosive nucleosynthesis (Weaver & Woosley 1993).

3.5. *Iron*

There exists very little information on iron abundance in supergiant H II regions in galaxies. This is due, in part, to the weakness of iron lines in H II region spectra, but also to the uncertainties in the atomic data concerning iron ions.

Thanks to the high signal-to-noise ratio of our spectra, the [Fe III] λ4658 line was detected with good precision in seven BCGs from our sample. In addition, the [Fe III] λ4986 and [Fe III] λ5271 lines were also seen in a few galaxies. In addition to the uncertainty in the atomic data, there are other uncertainties connected with iron abundance determination. First, the [Fe III] λ4658 line which is used to derive iron abundance can be blended with broad Wolf-Rayet features such as C III/C IV λ4650 and N III/N IV λ4640. In the BCGs where this happens (1135+581, 1437+370), the Wolf-Rayet contribution has been carefully substracted from the [Fe III] λ4658 line. Second, in the type of galaxies studied here, iron is mostly in the Fe^{+3} stage while we observed only lines of Fe^{++}, whose fraction does not exceed 10% (Stasinska 1990). However, the Fe^{++} zone coincides well with the O^+ zone, so we can make use of the O/O^+ ratio to correct for the unseen iron ionization stages (eq. [16]). Using the emissivities of Garstang et al. (1978) for the [Fe III] λ4658 line, we derived the iron abundances relative to oxygen listed in Table 5. We note the small dispersion in the Fe/O ratio. The mean weighted value is $\langle \log \mathrm{Fe/O} \rangle = -1.74 \pm 0.10$. Again, Fe/O is roughly constant and does not depend on O/H, suggesting that both O and Fe are made by the same massive stars.

It is interesting to compare the iron-to-oxygen abundance ratio of BCGs to that of galactic stars. It is common practice to express element abundances in stars relative to Fe abundance in terms of overabundance with respect to the Sun. Thus [A/Fe] gives the overabundance with respect to the Sun of element A relative to iron. For the solar oxygen abundance, we adopt $N(\mathrm{O})_\odot = 8.91$ (Anders & Grevesse 1989; Meyer 1989). There is some uncertainty concerning the solar iron abundance. Anders & Grevesse (1989) give $N(\mathrm{Fe})_\odot = 7.66$, which differs significantly from the meteoritic value of 7.51. However, new determinations of the solar iron abundance based on new values of Fe I and Fe II oscillator strengths are consistent with the meteoritic value (Holweger et al. 1991; Biémont et al. 1991; Hannaford et al. 1992), which we adopt.

We show in Figure 6 the dependence of [O/Fe] on [Fe/H] for the BCGs in our sample (*filled points*). For comparison, we also plot the scarce existing Fe data on H II regions in other galaxies: that of 30 Doradus in the Large Magellanic Cloud (*filled star*; Rosa & Mathis 1987) and that of the Orion nebula (*open star*; Osterbrock et al. 1992). We have also shown the data for galactic disk stars from Edvardsson et al. (1993) (*open triangles*), and for galactic halo and disk stars from Barbuy

© American Astronomical Society • Provided by the NASA Astrophysics Data System

1995ApJ...445..108T

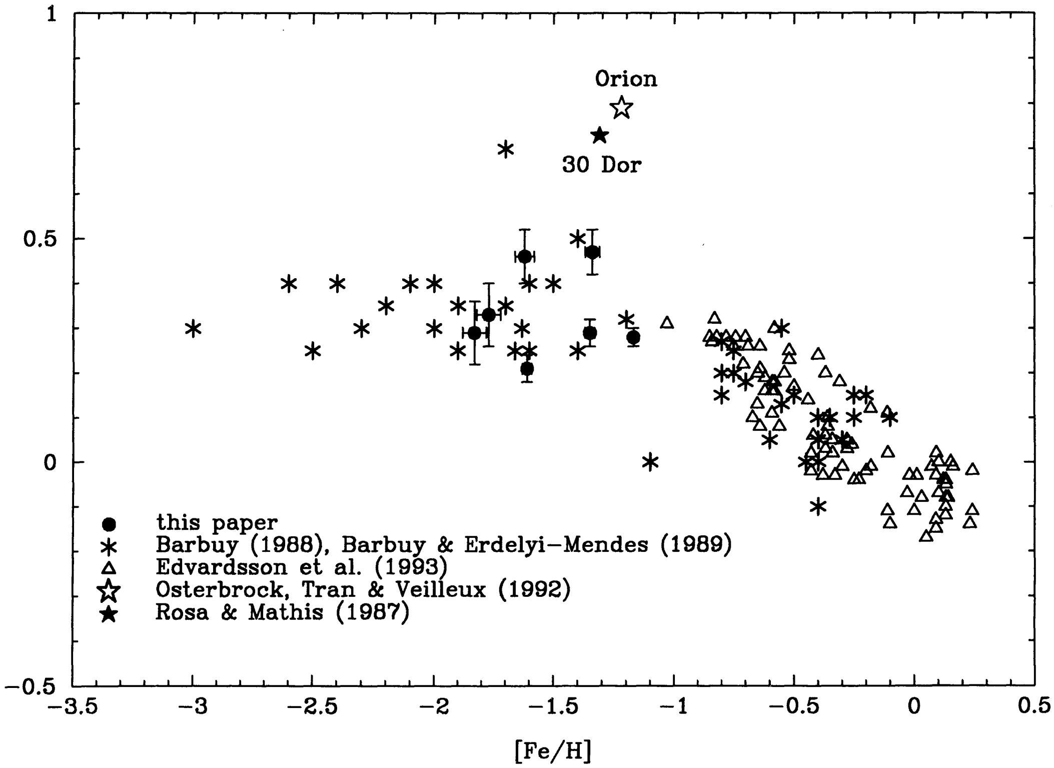

FIG. 6.—Overabundance of oxygen relative to iron [O/Fe] with respect to the Sun, as a function of metallicity [Fe/H] for seven BCGs in our sample (*filled circles*). For comparison, we have also shown the data for disk stars from Edvardsson et al. (1993; *open triangles*), for disk and halo stars from Barbuy (1988) and Barbuy & Erdelyi-Mendes (1989; *asterisks*), for Orion (Osterbrock, Tran, & Veilleux 1992; *open star*) and 30 Doradus (Rosa & Mathis 1987; *filled star*). There is excellent agreement between the BCG data and that for galactic halo stars from Barbuy (1988) and Barbuy & Erdelyi-Mendes (1989), suggesting a similar chemical enrichment history.

(1988) and Barbuy & Erdelyi-Mendes (1989) (*asterisks*). Figure 6 shows an excellent agreement between the BCG data and those for halo stars ([Fe/H] < -1). For both types of objects, O/Fe is approximately constant implying that O and Fe are made by the same massive stars and is overabundant with respect to the Sun by a mean of ~ 0.34, reflecting the shorter timescale for the injection of oxygen and other α-elements into the ISM by SN II's, as compared to the injection timescale of Fe by SN I's. The agreement between the two types of objects prompts two remarks. First, it gives some confidence in our procedure of determining iron abundance with the use of emissivities for the [Fe III] $\lambda 4658$ line by Garstang et al. (1978) and of ionization correction factors by Stasinska (1990). Second, it says that ISM enrichment by supernovae in metal-deficient BCGs is very similar to that occurring in the halo of the Galaxy while it was collapsing. Because of the absence of zero-metallicity halo stars, it has been suggested that there has been early enrichment of the galactic halo by massive Population III stars. The similarity in [O/Fe] between BCGs and galactic halo stars supports this conjecture since massive stars are known to exist in BCGs. By contrast, galactic disk stars with [Fe/H] ≥ -1 show a progressive decrease toward the solar ratio, reflecting the gradual enrichment of the ISM of the galactic disk in Fe relative to O, mostly by SN I's, after disk formation.

The O/Fe ratio in Orion and in 30 Doradus (Fig. 6, *open* and *filled stars*) is significantly higher (by log O/Fe ~ 0.4) than in BCGs and halo stars. Osterbrock et al. (1992) attributed the high ratio in Orion to the depletion of iron caused by dust formation. If this is true, this mechanism appears to be not at work in the supergiant H II regions of BCGs.

4. COMPARISON OF OBSERVATIONAL DATA WITH THEORETICAL NUCLEOSYNTHETIC YIELDS FOR MASSIVE STARS

The main conclusion of the present study of heavy element abundances in BCGs is that enrichment of the ISM in supergiant H II regions is caused almost exclusively by massive stars. This is because none of the heavy element ratios N/O, Ne/O, S/O, Ar/O, or Fe/O shows any dependence on the O abundance, an element which is known to be made in massive stars ($M \geq 10\ M_\odot$), and in the case of N, because the dispersion of the N/O ratio is too small to allow any time-delay between N and O production. While this conclusion is hardly surprising for the α-elements Ne, S, and Ar, it is more so for primary N, which was thought to be made almost exclusively by intermediate-mass ($4\ M_\odot \leq M \leq 9\ M_\odot$) stars. We compare in this section the observed element abundance ratios in BCGs with theoretical yields to put constraints on parameters of current nucleosynthesis models of massive stars. The most extensive set of yield calculations for massive stars in the mass range $12\ M_\odot \leq M \leq 40\ M_\odot$ has been given by Weaver & Woosley (1993). Unfortunately, these models have been computed only for stars with solar metallicity $Z_\odot$, while our BCGs have $Z_\odot/35 \leq Z \leq Z_\odot/7$. However, we feel that, in view of the independence found in this work of the heavy element abundance ratios on the oxygen abundance (which is proportional

© American Astronomical Society • Provided by the NASA Astrophysics Data System

1995ApJ...445..108T

to the metallicity), the comparison of elemental abundances relative to oxygen to the results of solar metallicity models may be partly justified. Nevertheless, we caution the reader to take the following conclusions, derived from such a comparison, as just a zeroth-order approximation. More definitive statements will have to await the calculation of yields for metal-deficient massive stars.

Besides the metallicity problem, there are several uncertain parameters in these massive star models. First, the $^{12}C(\alpha, \gamma)^{16}O$ nuclear reaction rate, on which the produced amount of α-elements critically depends, is a function of the semiconvection rate. Weaver & Woosley (1993) have adjusted this rate to get the correct solar abundance ratios for intermediate-mass isotopes with atomic masses between 16 and 32. They found that, for plausible initial mass functions (IMF) good agreement between the heavy element yields of these models, and the observed solar abundance ratios can be obtained only if the rate of the $^{12}C(\alpha, \gamma)^{16}O$ reaction is taken to be 1.7 ± 0.5 times that given by Caughlan & Fowler (1988). These results are relatively insensitive to the IMF slope and to the particular theory of semiconvection. Second, the theoretical yields of elements produced during explosive nucleosynthesis (elements with atomic weights greater than 32, such as iron) are strongly dependent on the initial conditions of the explosion such as the mass of the collapsing core and/or the explosion energy (Woosley et al. 1993). Third, the heavy element yields are also dependent on the IMF and the stellar wind mass-loss rate.

In Table 6, we compare the abundances of heavy elements relative to oxygen as observed in our BCG sample with those predicted by various nucleosynthetic solar metallicity massive star models by Weaver & Woosley (1993). We have considered both single-mass models (15, 25, and 35 $M_\odot$) and models where stellar masses are distributed following an IMF with slope $\alpha = -1.5$ and -2.3, values that appear to bound the various observations. Here, α is defined by $dN/d(\log M) \propto M^\alpha$. For a given mass or IMF, and for all elements except iron, two types of models are taken into consideration: one labeled "1.7S" and the other labeled "1.7N." The notation "1.7" means that the $^{12}C(\alpha, \gamma)^{16}O$ reaction rate is taken to be 1.7 times that of Caughlan & Fowler (1988). "S" means that semiconvection is assumed to proceed at its "nominal" rate of 0.1 times the thermal diffusion rate, while "N" means that semiconvection proceeds at a "restricted" rate 1000 times smaller than the nominal rate. For iron, we have considered only single-mass (15, 25, and 35 $M_\odot$) explosive nucleosynthesis models of Weaver & Woosley (1993) with a $^{12}C(\alpha, \gamma)^{16}O$ reaction rate equal to 2 times that of Caughlan & Fowler (1988), and a nominal semiconvection rate (2.0S models). Inspection of Table 6 shows an excellent agreement between the observed abundances relative to oxygen for all elements except iron with those given by the 1.7S single-mass model for a 25 $M_\odot$ star. This unexpectedly good agreement gives us some confidence that our procedure of comparing observed elemental abundances relative to oxygen to those predicted by solar metallicity models may not be too unreasonable.

While, within the observational uncertainties, the agreement with the 1.7S model in the case where stellar masses are distributed following an IMF with slope $\alpha = -1.5$ or -2.3 is also acceptable, it is definitely worse than the single-mass case. Since the yield weighted mean mass for an IMF with slope -1.5 is only 17.2 $M_\odot$ and that for an IMF with slope -2.3 is 15.4 $M_\odot$, the slightly worse agreement may be an indication of a top-heavy IMF, with a somewhat shallower slope than a Salpeter or galactic slope in our metal-deficient BCGs. The very small dispersion in the observed N/O, Ne/O, S/O, Ar/O, and Fe/O abundance ratios also suggests that there cannot be large IMF variations between BCGs of different metallicities. Comparison of the observations with both S and N models shows a definite advantage in favor of the former, so that the "nominal" semiconvection rate appears to be more appropriate than the "restricted" rate.

The good agreement between the model theoretical yields for nitrogen and the mean observed nitrogen-to-oxygen abundance ratio in Table 6 is accidental. The N yields given in Table 6 were calculated with solar metallicity. In view of the secondary origin of N in the models of Weaver & Woosley (1993), the theoretical N/O yield ratio should decrease with decreasing initial metallicity. Because of the low metallicity ($Z_\odot/35 \leq Z \leq Z_\odot/7$) of the BCGs in our sample, Weaver & Woosley (1993) models should in fact predict a *smaller* N/O yield ratio than the observed abundance ratio. The then higher observed N/O ratio can be understood if nitrogen is fabricated in massive stars and is mainly of primary and not secondary origin, as discussed in § 3.3.

Iron is the only heavy element under study for which the theoretical yield is somewhat different from the observational

TABLE 6

COMPARISON OF OBSERVED HEAVY ELEMENT-TO-OXYGEN ABUNDANCE RATIOS WITH THEORETICAL HEAVY ELEMENT-TO-OXYGEN YIELD RATIOS FROM WEAVER & WOOSLEY 1993

Abundance	15 $M_\odot$		25 $M_\odot$		35 $M_\odot$		α=−1.5[a]		α=−2.3		
ratio	1.7S[b]	1.7N[b]	1.7S	1.7N	1.7S	1.7N	1.7S	1.7N	1.7S	1.7N	Observations
log(N/O)	−1.13	−0.56	−1.57	−1.26	−1.64	−1.53	−1.43	−1.16	−1.35	−1.06	−1.53±0.08
log(Ne/O) ..	−0.81	−0.62	−0.76	−1.39	−0.77	−0.76	−0.86	−0.81	−0.87	−0.80	−0.70±0.03
log(S/O)	−1.39	−0.71	−1.51	−1.29	−1.87	−1.65	−1.48	−1.37	−1.45	−1.27	−1.54±0.04
log(Ar/O) ..	−2.05	−1.40	−2.20	−1.96	−2.54	−2.32	−2.12	−2.05	−2.08	−1.96	−2.23±0.07
	2.0S[c]		2.0S[c]		2.0S[c]						
log(Fe/O) ..	−1.37	...	−1.37	...	−1.58	...	...	...	...	...	−1.74±0.10

[a] α = IMF slope of stellar mass distribution, defined by $dN/d(\log M) \propto M^\alpha$.

[b] 1.7S, 1.7N: nucleosynthesis models from Weaver & Woosley 1993 with a $^{12}C(\alpha, \gamma)^{16}O$ reaction rate 1.7 times that from Caughlan & Fowler 1988 and with a "nominal" semiconvection rate (S), or one reduced by a factor of 1000 (N).

[c] Explosive nucleosynthesis model from Weaver & Woosley 1993 with a $^{12}C(\alpha, \gamma)^{16}O$ reaction rate 2.0 times that from Caughlan & Fowler 1988, and a "nominal" semiconvection rate.

© American Astronomical Society • Provided by the NASA Astrophysics Data System

1995ApJ...445..108T

value. The predicted yields are about a factor of 2 higher than the observed values. However, this may not be significant as uncertainties in the theoretical yields, as estimated by Weaver & Woosley (1993), are also about a factor of 2. Besides the fact that Weaver & Woosley (1993) models are not quite appropriate for our metal-deficient BCGs because they were designed to match the solar Fe/O ratio, there are also uncertainties about the very physical processes which make iron.

^{56}Fe is the product of ^{56}Ni decay during the explosive nucleosynthesis of massive stars, and its yield is dependent on poorly known conditions during the supernova event. Woosley et al. (1993) have studied the sensitivity of ^{56}Ni production to the explosion energy and to the mass of the central collapsing core for a 60 $M_{\odot}$ star. They found little sensitivity to the former but a larger dependence on the latter. They calculated two different models: one with a mass cut of 1.403 $M_{\odot}$ at the edge of the iron core, and one with a mass cut of 1.552 $M_{\odot}$ at the base of the oxygen shell, where there is a large entropy jump. The second model, with a mass cut increase of just 10% above that of the first, has its ^{56}Ni production cut down in half, just about the factor needed to reconcile the theoretical Fe/O yield ratio in the 2.0S 25 $M_{\odot}$ model with the observational results. Thus, our observations suggest that the mass of the central collapsing core in explosive nucleosynthesis is somewhat larger ($\sim 10\%$) than the mass of the iron core.

5. CONCLUSIONS

We present in this paper high signal-to-noise ratio spectrophotometric observations of 15 H II regions in 14 low-metallicity blue compact galaxies selected mainly from the First and Second Byurakan surveys. We use these high-quality data to derive heavy element abundances, discuss their origin, and constrain current nucleosynthesis stellar models.

We have obtained the following main results:

1. The oxygen abundance in our BCGs ranges from $N(\mathrm{O}) = 7.37$ to 8.04. There are six galaxies in our sample with $Z \leq Z_{\odot}/15$, more than doubling the known number of very metal deficient BCGs. Our data constitute an excellent sample for studying heavy element abundances in a very low metallicity environment.

2. Abundances of the elements oxygen, nitrogen, neon, sulfur, and argon have been derived for all 15 H II regions and, for the first time in BCGs, iron for seven H II regions using ionization correction factors obtained from the grid of photoionized H II region models of Stasinska (1990). Correction for extinction and underlying stellar absorption was made over the whole spectral range, using the whole available Balmer line series, from Hα λ6563 to H12 λ3750.

3. The N/O, Ne/O, S/O, Ar/O, and Fe/O abundance ratios show no dependence on oxygen abundance and a very small dispersion. Given that oxygen is produced by massive ($M \geq 10$ $M_{\odot}$) stars, we conclude that, in low-metallicity BCGs all the above heavy elements are produced by the same massive stars, and *only* by these stars. While this conclusion is not surprising for α-elements such as Ne, S, and Ar, it is more so for N. The latter is thought to be produced in BCGs mainly as a primary element by intermediate-mass ($4\ M_{\odot} \leq M \leq 9\ M_{\odot}$) stars via dredge-up of hot-bottom burning carbon (Renzini & Voli 1981). However, because intermediate-mass stars have longer lifetimes than massive stars, there would be, in this scenario, a time delay between oxygen and nitrogen production, which would lead to a dispersion in the N/O abundance ratio larger than the observed value.

4. Relative to the Sun, log O/Fe in BCGs is overabundant by ~ 0.34, the same overabundance as found in galactic halo stars. This implies a similar chemical enrichment history for BCGs and the galactic halo and supports the scenario of an early enrichment of the galactic halo by massive Population III stars.

5. We have compared the observed heavy element abundances relative to oxygen with the theoretical yields of both hydrostatic and explosive nucleosynthesis stellar models with solar metallicity (Weaver & Woosley 1993). The independence of the heavy element abundance ratios on the oxygen abundance (and hence metallicity) may partly warrant such a comparison, although the following results are only a zeroth-order approximation. The best agreement was found for a 25 $M_{\odot}$ single-mass model, with a $^{12}\mathrm{C}(\alpha, \gamma)^{16}\mathrm{O}$ reaction rate 1.7 times the rate given by Caughlan & Fowler (1988), and with a "nominal" semiconvection rate of 0.1 times the thermal diffusion rate. The agreement is less good when the yields are integrated over an IMF with a Salpeter or galactic slope, suggesting perhaps top-heavy IMFs with slopes flatter than -1.5 in metal-deficient BCGs. The small dispersion in the heavy abundance ratios suggests also that there is *not* a large IMF variation between BCGs with different metallicities. Comparison of the observed and theoretical Fe/O yield ratio in BCGs favor explosive nucleosynthesis models where the mass of the central collapsing core is $\sim 10\%$ larger than the mass of the iron core.

T. X. T. acknowledges the partial financial support from Air Force Office for Scientific Research Grant AFOSR 89-0467, from a fellowship of the Ministère de la Recherche et de la Technologie and from a Visiting Professorship at the University of Paris VII. He is grateful to Chantal Balkowski and Laurent Vigroux for their warm hospitality respectively at the Observatoire de Meudon and the Centre d'Etudes de Saclay during his sabbatical year. This international collaboration has been made possible by the award of the 1992 Henri Chrétien Award by the American Astronomical Society and of NATO collaborative research grant 921285. Yu. I. I. has been supported in part by the Ukranian State Committee for Science and Technology and by grant A-02-037 of the ESO Central and Eastern European Programme. He thanks Chantal Balkowski for inviting him to Meudon. V. A. L. was supported in part by a grant from the US National Academy of Sciences. He thanks R. Green and the staff of NOAO for their kind hospitality. We are grateful to A. Kniazev and A. Ugryumov for their assistance with the processing of the spectra with the MIDAS software package, and we thank J.-P. Meyer, N. Prantzos, and G. Stasinska for informative discussions, and F. Timmes for helpful comments on the manuscript.

REFERENCES

Aller, L. H. 1984, Physics of Thermal Gaseous Nebulae (Dordrecht: Reidel)
Anders, E., & Grevesse, N. 1989, Geochim. Cosmochim. Acta, 53, 197
Arnett, W. D. 1978, ApJ, 219, 1008
Barbuy, B. 1988, A&A, 191, 121
Barbuy, B., & Erdelyi-Mendes, M. 1989, A&A, 214, 239
Bessel, M. S., Sutherland, R. S., & Ruan, K. 1991, ApJ, 383, L71
Biémont, E., Baudoux, M., Kurucz, R. L., Ansbacher, W., & Pinnington, E. H. 1991, A&A, 249, 539
Brocklehurst, M. 1971, MNRAS, 153, 471
Bruenn, S. W. 1989, ApJ, 340, 955

© American Astronomical Society • Provided by the NASA Astrophysics Data System

1995ApJ...445..108T

Burbidge, E. M., Burbidge, G. R., Fowler, W. A., & Hoyle, F. 1957, Rev. Mod. Phys., 29, 547
Cameron, A. G. W. 1957, Chalk River Report, CRL-41
Campbell, A., Terlevich, R., & Melnick, J. 1986, MNRAS, 223, 811
Caughlan, G. A., & Fowler, W. A. 1988, Atomic Data Nucl. Data Tables, 40, 238
Clegg, R. E. S., Lambert, D. L., & Tomkin, J. 1981, ApJ, 250, 262
Conti, P. S., Greenstein, J. L., Spinrad, H., Wallerstein, G., & Vardya, M. S. 1967, ApJ, 148, 105
Dufour, R. J., Garnett, D. R., & Shields, G. A. 1988, ApJ, 332, 752
Edvardsson, B., Andersen, J., Gustafsson, B., Lambert, D. L., Nissen, P. E., & Tomkin, J. 1993, A&A, 275, 101
Evans, I. N. 1986, ApJ, 309, 544
French, H. B. 1980, ApJ, 240, 41
Garnett, D. 1989, ApJ, 345, 282
———. 1990, ApJ, 363, 142
———. 1992, AJ, 103, 1330
Garstang, R. H., Robb, W. D., & Rountree, S. P. 1978, ApJ, 222, 384
Gratton, R. C., & Ortolani, S. 1986, A&A, 169, 201
Hannaford, P., Lowe, R. M., Grevesse, N., & Noels, A. 1992, A&A, 259, 301
Holweger, H., Bard, A., Kock, A., & Kock, M. 1991, A&A, 249, 545
Izotov, Yu. I., Guseva, N. G., Karachentsev, I. D., & Karachentseva, V. E. 1992a, Astron. Ap. Trans., 1, 283
Izotov, Yu. I., Lipovetsky, V. A., Guseva, N. G., Kniazev, A. Yu., Neizvestny, S. I., & Stepanian, J. A. 1992b, Astron. Ap. Trans., 3, 193
Izotov, Yu. I., Lipovetsky, V. A., Guseva, N. G., Kniazev, A. Yu., & Stepanian, J. A. 1990a, Nature, 343, 238
———. 1991, A&A, 247, 303
Izotov, Yu. I., Lipovetsky, V. A., Guseva, N. G., & Stepanian, J. A. 1990b, Pis'ma Astron. Zh., 16, 605
Izotov, Yu. I., Thuan, T. X., & Lipovetsky, V. A. 1994, ApJ, 435, 647 (Paper I)
Kinman, T. D., & Davidson, K. 1981, ApJ, 243, 147
Kunth, D., & Sargent, W. L. W. 1983, ApJ, 273, 81
Lambert, D. L., Sneden, C., & Ries, L. M. 1974, ApJ, 188, 97
Lequeux, J., Peimbert, M., Rayo, J. F., Serrano, A., & Torres-Peimbert, S. 1979, A&A, 80, 155
Maeder, A. 1992, A&A, 264, 105
Marconi, G., Matteucci, F., & Tosi, M. 1994, MNRAS, 270, 35
Markarian, B. E. 1967, Astrofizika, 3, 55
———. 1969, Astrofizika, 5, 443
Markarian, B. E., & Lipovetsky, V. A. 1972, Astrofizika, 8, 155
Markarian, B. E., Lipovetsky, V. A., & Stepanian, J. A. 1981, Astrofizika, 17, 619
———. 1983, Astrofizika, 19, 29
Markarian, B. E., Lipovetsky, V. A., Stepanian, J. A., Erastova, L. K., & Shapovalova, A. I. 1989, Comm. Special Ap. Obs., 62, 5
Matteucci, F., & Tosi, M. 1985, MNRAS, 217, 391
Mayle, R. W., & Wilson, J. R. 1988, ApJ, 334, 909
Melnick, J., Heydary-Malayeri, M., & Leisy, P. 1992, A&A, 253, 16
Meyer, J.-P. 1989, in Cosmic Abundances of Matter, ed. C. J. Waddington (New York: AIP), 245
Osterbrock, D. E., Tran, H. D., & Veilleux, S. 1992, ApJ, 389, 305
Pagel, B. E. J., & Edmunds, M. G. 1981, ARA&A, 19, 77
Pagel, B. E. J., Simonson, E. A., Terlevich, R. J., & Edmunds, M. G. 1992, MNRAS, 255, 325
Peña, M., Ruiz, M. T., & Maza, J. 1991, A&A, 251, 417
Pilyugin, L. S. 1992, A&A, 260, 58
———. 1993, A&A, 277, 42
Renzini, A., & Voli, M. 1981, A&A, 94, 175
Rosa, M., & Mathis, J. S. 1987, ApJ, 317, 163
Sanduleak, N., & Pesch, P. 1987, ApJS, 63, 809
Searle, L., & Sargent, W. L. W. 1972, ApJ, 173, 25
Serrano, A., & Peimbert, M. 1983, Rev. Mex. Astron. Af., 8, 117
Shaver, P. A., McGee, R. X., Newton, L. M., Danks, A. C., & Pottasch, S. R. 1983, MNRAS, 204, 53
Shields, G. A., Skillman, E. D., & Kennicutt, R. C. 1991, ApJ, 371, 82
Shigeyama, T., Nomoto, K., & Hashimoto, M. 1988, A&A, 196, 141
Skillman, E., & Kennicutt, R. C., Jr. 1993, ApJ, 411, 655
Spite, M., & Spite, F. 1991, A&A, 252, 689
Stasinska, G. 1990, A&AS, 83, 501
———. 1993, private communication
Stevenson, C. C., McCall, M. L., & Welch, D. L. 1993, ApJ, 408, 460
Terlevich, R., Melnick, J., Masegosa, J., Moles, M., & Copetti, M. V. F. 1991, A&AS, 91, 285
Thielemann, F.-K., Hashimoto, M., & Nomoto, K. 1990, ApJ, 349, 222
Thuan, T. X. 1991, in Massive Stars in Starbursts, ed. C. Leitherer, N. R. Walborn, T. M. Heckman, & C. A. Norman (Cambridge: Cambridge Univ. Press), 183
Thuan, T. X., Izotov, Yu. I., Lipovetsky, V. A., & Pustilnik, S. A. 1994, in Proc. of the ESO/OHP Workshop on Dwarf Galaxies, ed. G. Meylan & P. Prugniel (Garching: European Southern Observatory), 421
Thuan, T. X., & Martin, G. E. 1981, ApJ, 247, 823
Timmes, F. X. 1994, private communication
Tomkin, J., & Lambert, D. L. 1984, ApJ, 279, 220
Torres-Peimbert, S., Peimbert, M., & Fierro, J. 1989, ApJ, 345, 186
Vila-Costas, M. B., & Edmunds, M. G. 1993, MNRAS, 265, 199
Vigroux, L., Stasinska, G., & Comte, G. 1987, A&A, 172, 15
Vilchez, J. M., Pagel, B. E. J., Diaz, A., Terlevich, E., & Edmunds, E. 1988, MNRAS, 235, 633
Weaver, T. A., & Woosley, S. E. 1993, Phys. Rep., 227, 65
Wheeler, J. C., Sneden, C., & Truran, J. W., Jr. 1989, ARA&A, 27, 279
Woosley, S. E. 1988, ApJ, 330, 218
Woosley, S. E., Langer, N., & Weaver, T. A. 1993, ApJ, 411, 823
Woosley, S. E., & Weaver, T. A. 1982, in Supernovae: a Survey of Current Research, ed. M. J. Rees & R. J. Stoneham (Dordrecht: Reidel), 79
———. 1986, in Radiation Hydrodynamics in Stars and Compact Objects, ed. D. Mihalas & K. H. A. Winkler (Berlin: Springer), 91

© American Astronomical Society • Provided by the NASA Astrophysics Data System